Molecular Neurobiology (2019) 56:5167–5187
https://doi.org/10.1007/s12035-018-1442-9

Mitochondrial Neuroglobin Is Necessary for Protection Induced by Conditioned Medium from Human Adipose-Derived Mesenchymal Stem Cells in Astrocytic Cells Subjected to *Scratch* and Metabolic Injury

Eliana Baez-Jurado[1] · Gina Guio-Vega[1] · Oscar Hidalgo-Lanussa[1] · Janneth González[1] · Valentina Echeverria[2,3] · Ghulam Md Ashraf[4] · Amirhossein Sahebkar[5,6,7] · George E. Barreto[1]

Received: 26 September 2018 / Accepted: 29 November 2018 / Published online: 8 December 2018

Abstract

Astrocytes are specialized cells capable of regulating inflammatory responses in neurodegenerative diseases or traumatic brain injury. In addition to playing an important role in neuroinflammation, these cells regulate essential functions for the preservation of brain tissue. Therefore, the search for therapeutic alternatives to preserve these cells and maintain their functions contributes in some way to counteract the progress of the injury and maintain neuronal survival in various brain pathologies. Among these strategies, the conditioned medium from human adipose-derived mesenchymal stem cells (CM-hMSCA) has been reported with a potential beneficial effect against several neuropathologies. In this study, we evaluated the potential effect of CM-hMSCA in a model of human astrocytes (T98G cells) subjected to *scratch* injury. Our findings demonstrated that CM-hMSCA regulates the cytokines IL-2, IL-6, IL-8, IL-10, GM-CSF, and TNF-α, downregulates calcium at the cytoplasmic level, and regulates mitochondrial dynamics and the respiratory chain. These actions are accompanied by modulation of the expression of different proteins involved in signaling pathways such as AKT/pAKT and ERK1/2/pERK, and may mediate the localization of neuroglobin (Ngb) at the cellular level. We also confirmed that Ngb mediated the protective effects of CM-hMSCA through regulation of proteins involved in survival pathways and oxidative stress. In conclusion, regulation of brain inflammation combined with the recovery of fundamental cellular aspects in the face of injury makes CM-hMSCA a promising candidate for the protection of astrocytes in brain pathologies.

Keywords Astrocytes · *Scratch* assay · Mesenchymal stem cells · Inflammation · Conditioned medium · Neuroglobin

Electronic supplementary material The online version of this article (https://doi.org/10.1007/s12035-018-1442-9) contains supplementary material, which is available to authorized users.

✉ George E. Barreto
gsampaio@javeriana.edu.co; gesbarreto@gmail.com

[1] Departamento de Nutrición y Bioquímica, Facultad de Ciencias, Pontificia Universidad Javeriana, Bogotá, D.C., Colombia

[2] Facultad de Ciencias de la Salud, Universidad San Sebastian, Lientur 1457, 4080871 Concepción, Chile

[3] Research & Development Service, Bay Pines VA Healthcare System, Bay Pines, FL 33744, USA

[4] King Fahd Medical Research Center, King Abdulaziz University, Jeddah 21589, Saudi Arabia

[5] Neurogenic Inflammation Research Center, Mashhad University of Medical Sciences, Mashhad, Iran

[6] Biotechnology Research Center, Pharmaceutical Technology Institute, Mashhad University of Medical Sciences, Mashhad, Iran

[7] School of Pharmacy, Mashhad University of Medical Sciences, Mashhad, Iran

Introduction

Brain pathologies such as stroke, ischemia, amyotrophic lateral sclerosis (ALS), neurodegeneration, and traumatic brain injury (TBI) all share an inflammatory component in their etiology. The brain is a privileged organ from the immune point of view [1]. Different cells that make up the brain tissue are able to respond as sensors to any variation in the environment by regulating cellular processes. Of these cells, astrocytes and microglia directly regulate neuroinflammatory processes [2–4] by generating biochemical and cellular responses. Such responses are diverse and can range from the regulation of calcium levels in different cellular compartments to the expression of proteins involved in signaling pathways that may lead to a continuous and systematic deterioration of brain tissue [5, 6]. Hitherto, several molecules and therapeutic alternatives have been assessed as an attempt to reduce the impact of inflammatory markers, oxidative stress, and cell death in the face of central nervous system (CNS) lesions.

The use of conditioned medium-mesenchymal stem cells derived from human adipose tissue (CM-hMSCA) has shown a wide range of neuroprotective effects [7–10], which are mainly attributed to secreted molecules and soluble factors such as neurotrophins, cytokines, anti-inflammatory molecules, and anti-apoptotic molecules [11]. CM-hMSCA can affect different cellular processes and provide cytoprotective and immunomodulatory effects. For this reason, CM-hMSCA has been considered as a possible therapeutic alternative for the treatment or prevention of secondary injury caused by the inflammatory processes that develop during cerebral pathologies [7, 8, 12]. Notably, CM-hMSCA is promising in cell therapy not only for the benefits that had previously been reported [9, 10, 13–15] but also because these cells are derived from adipose tissue which is an abundant and easily accessible source of MSCs [16, 17].

Previous studies have reported the efficacy of CM-hMSCA to improve wound closure, to reduce the production of reactive oxygen species (ROS) [18], and to protect the mitochondrial ultrastructure of scratched astrocytes [9, 10]. Moreover, CM-hMSCA provides cytoprotection of astrocytes in different cerebral pathologies such as ischemia [19], oxygen and glucose deprivation (OGD) [20], and ALS [21]. It is possible that CM-hMSCA can modulate astrocytes signaling proteins or the expression of protective proteins in case of cellular damage. Previously, we showed an increase in neuroglobin (Ngb) expression in cells exposed to 2% CM-hMSCA [10]. Ngb is an oxygen-related protein involved in cerebral homeostasis and responsible for the detection and elimination of ROS [22–26]. Ngb is expressed by astrocytic cells and is upregulated under glucose deprivation [27, 28].

There is strong evidence on the upregulation of Ngb in astrocytes after hypoxic-ischemic lesions and TBI [29–31]. These findings suggest that neuroglobin may play an important role in mediating possible neuroprotection under pathological conditions. However, the mechanisms of action of CM-hMSCA and Ngb in protecting astrocytes during TBI have not been fully explored. For this reason, we investigated the possible mechanisms of action of CM-hMSCA in astrocytic cells exposed to a mechanical injury (*scratch*) and glucose deprivation, as well as the effect that CM-hMSCA might have on the regulation of cytokines, cytoplasmic calcium levels, regulation of mitochondrial dynamics, and/or the expression of proteins of interest in cell survival. In addition, we investigated the subcellular localization of Ngb and whether blocking this protein is related to the dynamics of calcium and other mitochondrial functions.

Materials and Methods

Primary Culture of Mesenchymal Stem Cells Derived from Human Adipose Tissue (hMSCA)

hMSCA were isolated as described elsewhere [32]. The procedures were performed according to a protocol approved by the Ethics Committee of the Pontificia Universidad Javeriana. Briefly, hMSCA were obtained from human adipose tissue by liposuction in patients between 24 and 28 years of age. hMSCA were characterized by assessing the expression of CD34(−), CD73(+), CD90(+), and CD105(+) following the criteria established by the International Society for Cell Therapy. hMSCA cells were cultivated in Dulbecco's modified Eagle's medium (DMEM) (LONZA, Walkersville, USA) supplemented with 10% fetal bovine serum (FBS) (LONZA, Walkersville, USA) and 1% penicillin, with an incubation temperature of 37 °C and 5% CO_2.

Preparation of CM-hMSCA

hMSCA were cultured until 80% confluency in Dulbecco's modified Eagle medium (DMEM) supplemented with 10% FBS. Then, the cells were cultured in serum- and glucose-free DMEM, and the conditioned medium was collected after 48 h. The supernatants were centrifuged at 3000 rpm for 3 min and stored at − 80 °C. CM-hMSCA were collected from hMSCA cultures between passages III and V.

T98G Cell Culture

T98G (ATCC CRL-1690) is a human cell line positive for GFAP [33]. This line has been used and validated as a model of astrocytic cells as reported previously [34–36]. Additionally, our group observed that these cells have characteristics similar to those of human astrocytes from primary cultures (data not shown). Cells were maintained under exponential growth in DMEM (LONZA) containing 10% FBS (LONZA) and 10 U penicillin/10 μg streptomycin/25 ng amphotericin (LONZA). The culture medium was changed three times a week. Cultures were incubated at 37 °C in a humidified atmosphere containing 5% CO_2.

Scratch Assay and CM-hMSCA Treatments

In this study, our in vitro model (*scratch* assay) was characterized by both mechanical injury and metabolic insult. As we did not observe mitochondrial damage in cells subjected to mechanical injury alone, we induced a metabolic impairment (glucose deprivation, BSS0) to simulate a previously

described traumatic brain like-injury model [18]. Briefly, cells were allowed to reach confluence for 48 h and then were serum deprived for 3 h. Later, a denuded area was produced by scratching the inside diameter of the well with the 10-μl pipette tip [18, 37]. Immediately after the *scratch*, the cells were rinsed twice with phosphate-buffered saline (PBS) 1× buffer to remove debris and were co-treated according to the following experimental groups: (1) *scratch* + BSS0, cells under *scratch* and glucose-free conditions (BSS0); (2) *scratch* + BSS5, *scratch* cells plus BSS0 supplemented with 5.5 mM glucose (BSS5, control cells); (3) *scratch* + BSS0 + CM2%, *scratch* cells plus BSS0 and treated with 2% CM-hMSCA; and (4) *scratch* + BSS5 + CM2%, *scratch* cells plus BSS5 and treated with 2% CM-hMSCA. Glucose deprivation assay was performed as previously reported [33, 38], and the composition of the balanced salt solution (BSS0) was NaCl, 116; $CaCl_2$, 1.8; $MgSO_4$ (7·H_2O), 0.8; KCl, 5.4; NaH_2PO4, 1; $NaHCO_3$, 14.7; and 4-(2-hydroxyethyl)-1-piperazineethanesulfonic acid (HEPES), 10; pH 7.4 to 37 °C. In this study, cells were subjected to *scratch* assay (mechanical injury + glucose deprivation) and simultaneously received a treatment with 2% CM-hMSCA for 24 h. This concentration of CM-hMSCA was chosen based on the findings of our previous study [10, 18].

Determination of Cytokines

Cells were treated according to the different experimental groups described in "*Scratch* Assay and CM-hMSCA Treatments." At the end of the experimental time, the supernatants of each group were collected and evaluated using the Human Inflammatory Cytokines Multi-Analyte ELISArray™ Kits - Multi-Analyte ELISArray Kit (SABiosciences MD, USA. Catalog #MEM-004A). The cytokine assay was performed taking into account the conditions and times referred to in the manufacturer's instructions. Briefly, this kit uses highly specific antibodies to detect cytokines in multiple samples. Heatmap visualizations were generated using GraphPad Prism version 7 for Windows. Differentially expressed cytokines were identified using one-way ANOVA test.

Determination of Cellular Calcium (Ca^{2+})

For the determination of cellular Ca^{2+}, cells were seeded at a density of 40,000 cells per well into 48-well plates in DMEM culture medium containing 10% FBS. After 48 h, the cells were treated according to each experimental paradigm on the second day. Specifically, for each labeled calcium indicator, the manufacturer's specifications and recommendations were followed. Briefly, for the cytoplasmic Ca^{2+} ($[Ca^{2+}]_{cyto}$), the cells were loaded with 3 μM Fluo-4 AM (Invitrogen, F-14217); for the case of mitochondrial Ca^{2+} ($[Ca^{2+}]_{mito}$), the cells were loaded with 5 μM Rhod-2 AM (Invitrogen, R1244); and for the case of the Ca^{2+} endoplasmic reticulum ($[Ca^{2+}]_{ER}$), the cells were loaded with 3 μM Mag-fura-2-AM (Invitrogen, M1291), with an incubation of 30 min at 37 °C for each indicator. Then, the reading was performed using a FLUOstar Omega multi-mode microplate reader (BMG LABTECH, Ortenberg, Germany) with a label (Ex/Em of Ca^{2+}-bound form): Fluo-4, AM (485/520); Rhod-2, AM (540/570 nm), and Mag-fura-2, AM (390/510) and with a scan width [mm]: 9, a setting time: 0,2 seg, and 20 flashes scan point. Each trial was performed with a minimum of eight replicates for each condition. The experiment was repeated three times.

Reverse Transcription

After subjecting the cells to different experimental procedures for 24 h, RNA was isolated from the cultures using Trizol (Invitrogen; 15596026), according to the manufacturer's instructions and as previously reported [39]. The RNA was resuspended in 50 μl of RNase- and DNase-free H_2O, and stored at − 80 °C. Then, a treatment with DNase I (RNase-Free) was performed to eliminate traces of DNA present in the extraction test following the manufacturer's instructions (Biolabs, M0303S). RNA concentration was determined using the NanoDrop (TM) 1000 UV/VIS spectrophotometer (Thermo Fisher). OD ratios of 260/280 nm close to 2.0 were obtained for all of the samples, indicating high purity. To obtain the complementary DNA (cDNA), the RNA was first normalized at 400–500 ng/μl with RNase- and DNase-free H_2O. To 11 μl of normalized RNA, 1 μl of Oligo d(T)18 mRNA Primer (Invitrogen™; SO131) and 1 μl of dNTPs Mix (2.5 nM) (Bioline, BIO-39029) were added. This mixture was pre-incubated at 65 °C for 5 min, leaving it immediately after ice. Subsequently, the reaction was completed with 4 μl of 5X First-Strand Buffer [250 mM Tris-HCl (pH 8.3), 375 mM KCl, 15 mM MgCl], with 2 μl DTT (0.1 M) and 1 μl of the M-MLV Reverse Transcriptase (200 U/μl) (Invitrogen™, Cat. 28025013) at the final volume of 20 μl. The reaction mixtures were incubated at 37 °C for 50 min and then at 70 °C for 15 min for the inactivation of the enzyme in a MasterCycler Gradient Thermal Cycler.

Real-Time PCR Evaluation

The levels of the evaluated genes were analyzed by the QuantStudio ™ 3 Real-Time PCR System (Applied Biosystems). We analyzed genes involved in mitochondrial dynamics (*mnf1-mnf2-fis1-Drp1-opa1*) as well as ND1 and ND2 present in the respiratory chain. Forward and reverse primers for the specific amplification of genes were selected through the Primer Bank database and a basic local alignment search tool (BLAST, NCBI) to confirm the target gene. The

primers were synthesized by Integrated DNA Technologies (IDT). The sequences used are shown in Table 1. Subsequently, 1 μl of cDNA from the controls and from the treated cells obtained after reverse transcription was completed to the final volume of 10 μl with Power SYBR® Green PCR Master Mix (1X) (Applied Biosystems; 4367659), forward and reverse for each gene of interest (400 nM) and the rest with RNase- and DNase-free H_2O. The protocol for the QuantStudio™ 3 Real-Time PCR System consists of a step of denaturation at 95 °C for 2 min, then 40 cycles of 10 s at 95 °C and 10 s at the optimal hybridization temperature of each gene (60 °C for *mfn1*, *opa1*, *Drp1*, *fis1*, ND2, ND1, and *GAPDH*, and 58 °C for *mnf2*), 20 s at 72 °C, and 10 s at 95 °C. Then, to obtain melting curves for the resulting PCR products, added temperature increase cycles from 70 to 95 °C by 0.15 °C/s. The relative quantification of the PCR products was carried out using the comparative method C_t [40] and as a relation between the control gene (GAPDH) and the signal of the gene of interest. To ensure data quality, all tests were performed in duplicate. The experiments were repeated at least three times.

Protein Extraction and Western Blotting

T98G cells were lysed on ice with RIPA Lysis and Extraction Buffer Thermo Scientific™ supplemented with Halt™ Protease Inhibitor Cocktail, EDTA-free (100X) (Cat #87785). Protein content was estimated using the Pierce™ BCA Protein Assay Kit. Equal amounts of protein were dissolved in sample buffer containing 5% β-mercaptoethanol and boiled. Then, the proteins were separated by electrophoresis in SDS–PAGE, transferred onto a PVDF membrane, and blocked in 5% skim milk dissolved in Tris-buffered saline containing 0.05% Tween 20 (TBS-T), at room temperature (RT) for 1 h. The membranes were incubated at 4 °C overnight with antibodies against neuroglobin (Ngb) (sc-133,086) (1:100), β-actin (Cat #MA1-140) (1:3000), superoxide dismutase 2 (SOD2) (Cat #PA5-30604) (1:1000), catalase (Cat #PA5-29183) (1:1000), GPX1 (Cat #PA5-30593) (1:1500) and AKT (Cat #PA5-31915), p-AKT (Cat #44-621G), ERK1/2 (Cat #44-654G), and p-ERK (Cat # 700012) (1:1000). The immunoreactivity was visualized by incubating the membrane with specific secondary antibody (IRDye® Antibodies) for 1 h and detected using Odyssey CLx Imaging System Specifications (LI-COR Biosciences). The images were analyzed using the Odyssey application software, version 1.2 (Li-Cor), to obtain the integrated intensities. All data were normalized to control values on each gel. We used the histogram method to analyze and standardize the densitometric data, and also based on previous reports to refine the methodology [41, 42].

Mitochondrial Inhibition in Cell Culture

For mitochondrial inhibition experiments, cells were seeded at a density of 40,000 cells per well into 48-well plates. The cultures were treated according to the experimental paradigm and in the presence of 2 μM of antimycin A (AA) (Sigma, A8674) as previously reported [43, 44]. We performed a time curve (0, 2, 8, 12, 18, and 24 h) to determine the response of the cells against the AA and determined viability by the MTT method, as previously reported by us [9]. Then, to confirm the inhibitory effect of AA, we assessed different mitochondrial functions. Experiments were performed in eight biological replicates and three independent trials.

Determination of ROS

ROS production was measured on a FLUOstar Omega multimode microplate reader (BMG LABTECH, Ortenberg, Germany) [45–47]. Briefly, cells were seeded at a density of 40,000 cells per well into 48-well plates in DMEM culture medium containing 10% FBS, and after 48 h, the cells were treated according to each experimental paradigm on the second day. To determine the effect of CM-hMSCA on the production of superoxide (O^{2-}), the cells were treated at a final concentration of 10 μM dihydroethidium (DHE) (Sigma, St Louis, MO, USA). The cultures were incubated for 15 min in the dark at 37 °C, and fluorescence was measured using exc485nm/emi570nm spectra and with a scan width [mm], 9; a setting time, 0,2 seg; and 20 flashes scan point. Each assay

Table 1 Information about primers used in the study

Gene	Primer sequences 5′–3′Forward	Primer sequences 5′–3′Reverse
Mfn1	GAGGTGCTATCTCGGAGACAC	GCCAATCCCACTAGGGAGAAC
Mfn2	CACATGGAGCGTTGTACCAG	TTGAGCACCTCCTTAGCAGAC
Drp1	CTGCCTCAAATCGTCGTAGTG	GAGGTCTCCGGGTGACAATTC
Fis1	GATGACATCCGTAAAGGCATCG	AGAAGACGTAATCCCGCTGTT
Opa1	ATTGAAGCTCTTCATCAGGAG	TGTATGCAGAGCTGATTATGAG
ND1	TCCTACTCCTCATTGTACCCA	TTTCGTTCGGTAAGCATTAGG
ND2	GTAAGCCTTCTCCTCACTCTC	TTAATCCACCTCAACTGCCT
GAPDH	CATCAATGGAAATCCCAT	TTCTCCATGGTGGTGAAGAC

was performed with a minimum of eight replicates for each condition. The experiment was repeated three times.

Determination of Mitochondrial Parameters

The mitochondrial membrane potential (Δψm) and the determination of active mitochondria through non-peroxidated cardiolipin [35, 48, 49] were the mitochondrial parameters evaluated. These determinations were assessed through the FLUOstar Omega multi-mode microplate reader (BMG LABTECH, Ortenberg, Germany). Briefly, for both determinations, the cells were seeded at a density of 40,000 cells per well into 48-well plates in DMEM culture medium containing 10% FBS and, after 48 h, the cells were treated according to each experimental paradigm on the second day.

Cells treated, or not, with 2% CM-hMSCA for 24 h were stained in the dark at 37 °C for 20 min with TMRM (Sigma, St Louis, MO, EE.UU.) (500 nM) for Δψm and acridine orange 10-nonyl bromide (NAO) (Sigma, St Louis, MO, EE.UU.) (200 nM) to determine the non-peroxidated cardiolipin. Data were obtained using excitation 540 nm/emission 570 nm spectra for TMRM and excitation 485 nm/emission 520 nm spectra for NAO and with scan width [mm] 9, a setting time 0,2 seg, and 20 flashes scan point. Each trial was performed with a minimum of eight replicates for each condition. The experiment was repeated three times.

Immunocytochemistry

Cells were washed with 0.1 M phosphate buffer (PB) and fixed in 4% paraformaldehyde for 30 min. Nonspecific binding sites were blocked with blocking buffer (3% bovine albumin and 0.3% Triton X-100) for 1 h. Subsequently, the cells were incubated overnight with the primary antibody for neuroglobin (Ngb) (sc-133,086) (1:100). After incubation with primary antibody, the cells were washed twice with PB and incubated with the appropriate secondary antibody goat anti-mouse IgG (H + L), DyLight 488 conjugate (Cat #35502) for 1 h and then analyzed using a High-Resolution Digital Camera—DP71 adapted to an Olympus BX51 microscope.

Co-localization Analysis

For co-localization analysis, double staining was performed using the Ngb antibody (green) and a construct used to transfect each organelle (red), according to BacMam 2.0 technology. The organelles were labeled for ≅ 24 h using CellLight® Mitochondria-RFP (C10601), Golgi-RFP (C10593), and ER-RFP (C10591) (Invitrogen), according to the manufacturer's instructions. Subsequently, the cells were treated according to the experimental paradigm and, after 24 h, the immunocytochemistry was performed for Ngb (see "Immunocytochemistry"). The assembly was made on slides, and then the photographic record was made in four different fields representing an area of 0.03 mm^2. The images were acquired with a high-resolution digital camera—DP71 adapted to an Olympus BX51 microscope.

For the co-localization analysis, the co-localization plugin Intensity Correlation Analysis 6.0 of ImageJ was used and this was made based on previous reports from our laboratory [33, 50]. In summary, the plugin generates a scatter plot plus correlation coefficients via Manders' coefficient. In each scatter plot, the first (channel 1, for example, red) image component is represented along the *x*-axis, the second image (channel 2, for example, green) along the *y*-axis. The intensity of a given pixel in the first image is used as the *x*-coordinate of the scatter-plot point and the intensity of the corresponding pixel in the second image as the *y*-coordinate, so the presence of yellow spots in the scatter indicated the co-localization frequency [51].

Dispersion diagrams were used to filter the co-localization of Ngb in each organelle. Using the plugin Intensity Correlation Analysis 6.0 of ImageJ, an image of co-localized pixels and also an image of those co-localized pixels superimposed on RGB-merge of two 8-bit images were generated. Finally, the co-localization finder algorithm was used to prompt two gray-scale images and creates a scatter plot and a red-green merged image. The pixels represented by the scatter plot point can be highlighted by selecting the points with the rectangular selection tool only [51]. As a result of this process, the percentage of co-localization for each microphotograph was obtained. Four microscope fields were analyzed in 20 images for each condition. The results were plotted as a percentage of co-location.

Neuroglobin Silencing

Cells were transfected in a serum-free condition with either Stealth RNAi™ Ngb siRNA (siNgb; Invitrogen, Carlsbad, CA, USA) or a mismatch sequence in accordance with the manufacturer's instructions, using oligofectamine (Invitrogen) as the transfection reagent. The sequence used for Ngb oligonucleotides was 5′-CGUGAUUGAUGCUGCAGUGACCAAU-3′. The mismatch sequence used as a control for Ngb siRNA (siNgb) was 5′-UGUGAUUUAUGGUGCAGUAACCAAC-3′. Briefly, oligofectamine and oligonucleotides (400 pM) were mixed with Optimem, and the mixture was incubated for 20 min at RT, diluted with Optimem, and added to the cell medium for 4 h at 37 °C. The medium was added to cells to reach the growing conditions (i.e., 10% (*v*/*v*) serum). To evaluate the effective silencing of Ngb, total proteins were extracted 48 h after transfection, and Ngb expression was assessed by western blot analysis.

Statistical Analysis

The GraphPad Prism version 6.0 for Windows (GraphPad Software, La Jolla, CA, USA) (www.graphpad.com) was

used for all statistical analyses. Data obtained from this study were tested for normal distribution using Kolmogorov–Smirnov test and for homogeneity of variance using Levene's test. Then, data were compared using analysis of variance (ANOVA) followed by Dunnet's post hoc test for comparisons between controls and treatments, and Tukey's post hoc test for multiple comparisons between the means of treatments and time points. Data are presented as mean ± SEM of three independent experiments. A statistically significant difference was defined at $p < 0.05$.

Results

Effect of CM-hMSCA on the Secretion of Cytokines in the Astrocytic Model Subjected to *Scratch* Assay

Previously, we reported that 2% CM-hMSCA was able to protect astrocytic cells under *scratch* assay. This in vitro model is characterized by both mechanical injury and glucose deprivation [10, 18]. We initially assayed cytokines using ELISA kits to profile the inflammatory responses of scratched astrocytic cells following treatment with CM-hMSCA (Fig. 1). An increase in the expression of the cytokines IL-6 (9.05%), TNF-α (3.8%), and GM-CSF (86.4%) was observed in cells subjected to *scratch* + BSS0 versus control (*scratch* + BSS5) cells (Fig. 1). Interestingly, our results showed a significant decrease of these cytokines in cells subjected to *scratch* + BSS0 + CM2% for 24 h. The reduction of these cytokines was around 17.8%, 27.3%, and 33.3% for IL-6, TNF-α, and GM-CSF, respectively, compared to the *scratch* + BSS0 cells (Fig. 1). Other cytokines such as IL-2 and IL-8 were elevated by 26% and 95%, respectively, in *scratch* + BSS0 + CM2% cells compared to *scratch* + BSS0 cells (Fig. 1). Nevertheless, no significant difference in the regulation of IL-10 was observed when cells were subjected to *scratch* + BSS0 + CM2% (Fig. 1).

2% CM-hMSCA Regulates Calcium (Ca^{2+}) Levels in the Astrocytic Model Subjected to *Scratch*

We evaluated the effect of 2% CM-hMSCA on calcium levels (Ca^{2+}) (Fig. 2) at different time periods (0, 6, and 24 h). Ca^{2+} was evaluated in the cytoplasm ($[Ca^{2+}]_{cyto}$) (Fig. 2a), mitochondria ($[Ca^{2+}]_{mito}$) (Fig. 2b), and endoplasmic reticulum ($[Ca^{2+}]_{ER}$) (Fig. 2c). *Scratch* + BSS0 + CM2% cells increased $[Ca^{2+}]_{cyto}$ by 25% at 0 h and 16% for 6 h versus *scratch* + BSS0, and these levels were similar to *scratch* + BSS5 cells (control) (Fig. 2a). In $[Ca^{2+}]_{mito}$ (Fig. 2b) and $[Ca^{2+}]_{ER}$ (Fig. 2c), no significant difference was observed at 0 and 6 h. At 24 h, cells exposed to *scratch* + BSS0 showed a significant increase of 23.8% in $[Ca^{2+}]_{cyto}$ versus the control (*scratch* + BSS5) (Fig. 2a) while $[Ca^{2+}]_{cyto}$ was found to be significantly decreased by 15.1% in *scratch* + BSS0 + CM2% cells (Fig. 2a). Moreover, at 24 h, $[Ca^{2+}]_{mito}$ increased significantly by 16.1% in *scratch* + BSS0 + CM2% cells (Fig. 2b), while $[Ca^{2+}]_{ER}$ only showed a slight and non-significant increase (6%) in the injured cells (*scratch* + BSS0) (Fig. 2c).

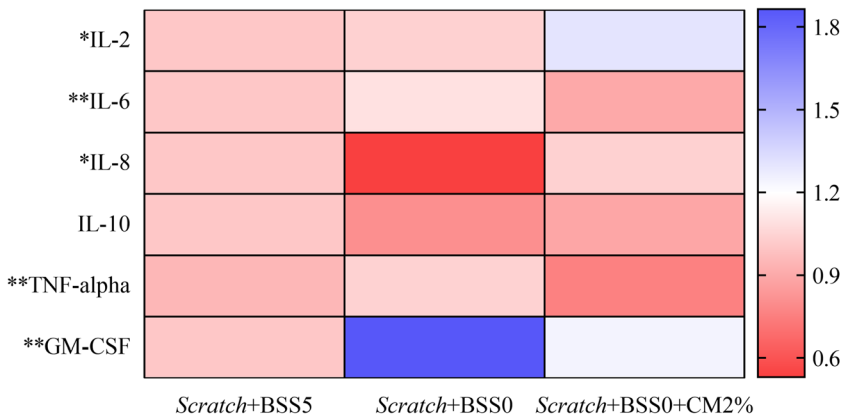

Fig. 1 Heat map of the profile of cytokine secretion in an astrocytic model subjected to *scratch* test. The cytokine profile is shown 24 h after co-treatment. Dark blue means greater presence and dark red denotes lower levels. Briefly, the *scratch* + BSS0 assay increased the secretion of IL-6 (*scratch* + BSS0 vs. *scratch* + BSS5, $p = 0.0173$), TNF-α (*scratch* + BSS0 vs. *scratch* + BSS5, $p = 0.0387$), and GM-CSF (*scratch* + BSS0 vs. *scratch* + BSS5, $p < 0.0001$), indicated in the heat map in dark pink and dark blue, respectively. 2% CM-hMSCA decreased cytokine secretion induced by the *scratch* assay: IL-6 (*scratch* + BSS0 + CM2% vs. *scratch* + BSS0, $p < 0.0001$), TNF-α (*scratch* + BSS0 + CM2% vs. *scratch* + BSS0, $p < 0.0001$), and GM-CSF (*scratch* + BSS0 + CM2% vs. *scratch* + BSS0, $p < 0.0001$), indicated in the heat map in dark pink. In addition, 2% CM-hMSCA regulated upwards cytokines such as IL-2 (*scratch* + BSS0 + CM2% vs. *scratch* + BSS0, $p < 0.0001$) and IL-8 (*scratch* + BSS0 + CM2% vs. *scratch* + BSS0, $p < 0.0001$), indicated in the white and pale pink heat map, respectively. One asterisk indicates cytokines with significant increase and two asterisks indicate cytokines with significant decrease in *scratch* + BSS0 + CM2% vs. *scratch* + BSS0 cells

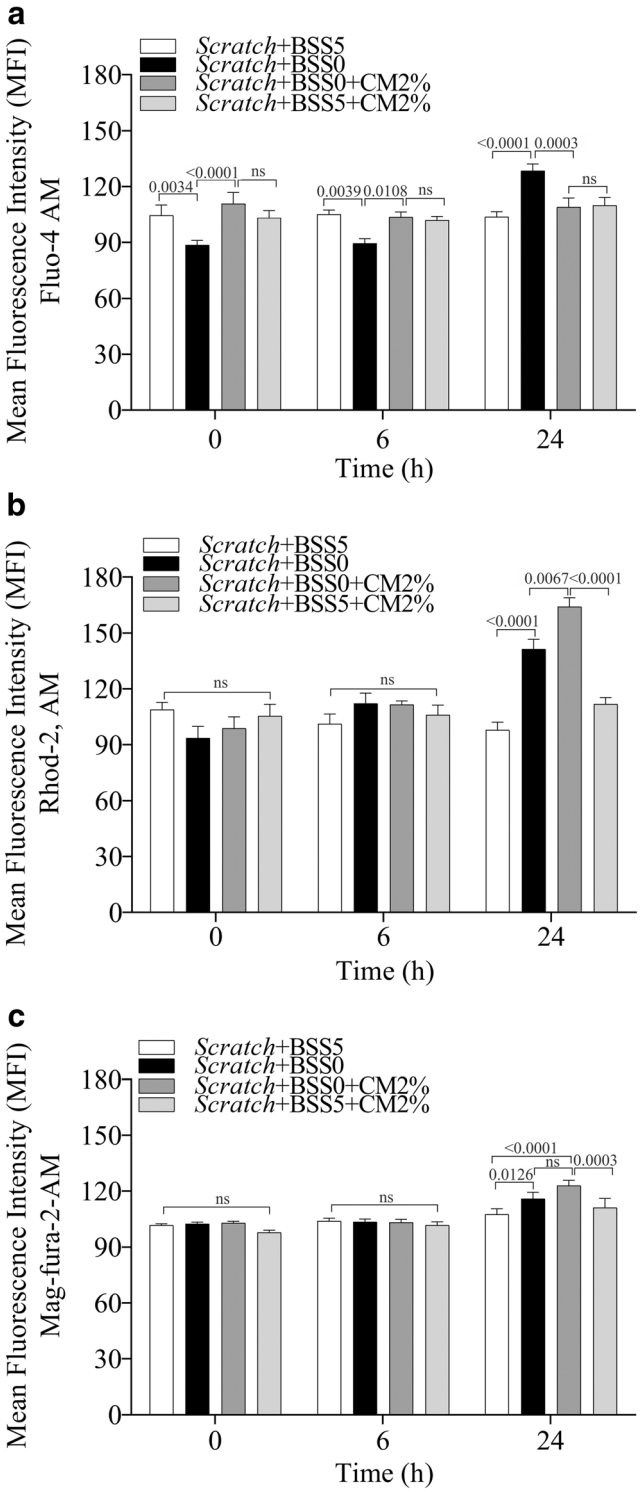

◀ **Fig. 2** CM-hMSCA regulates calcium (Ca^{2+}) levels in scratch cells exposed to CM2% at different times. The bar graphs show the percentages of fluorescence mean intensity (IMF) for Fluo 4-AM of $[Ca^{2+}]_{cyto}$ (**a**), Rhod-2 of $[Ca^{2+}]_{mito}$ (**b**), and MagFura of $[Ca^{2+}]_{ER}$ (**c**). The data are represented as the mean ± SEM of three experiments. In the initial times (0 h) there was an increase of $[Ca^{2+}]_{cyto}$ (*scratch* + BSS0 + CM2% vs. *scratch* + BSS0, $p < 0.0001$) and also at 6 h (*scratch* + BSS0 + CM2% vs. *scratch* + BSS0, $p = 0.0108$), but these values were not significant compared to the control (*scratch* + BSS5; $p = 0.4722$ (0 h); $p = 0.9832$ (6 h)). At 24 h, the *scratch* + BSS0 increases the $[Ca^{2+}]_{cyto}$ (*scratch* + BSS0 vs. *scratch* + BSS5, $p < 0.0001$), but in *scratch* + BSS0 + CM2% cells these levels are significantly reduced (*scratch* + BSS0 + CM2% vs. *scratch* + BSS0, $p < 0.0003$) (**a**). The levels of $[Ca^{2+}]_{ER}$ tended upwards in cells exposed to *scratch* + BSS0 + CM2%, but without significant differences at 24 h (*scratch* + BSS0 + CM2% vs. *scratch* + BSS0, $p = 0.0536$) (**c**). The $[Ca^{2+}]_{mito}$ increased significantly (*scratch* + BSS0 + CM2% vs. *scratch* + BSS0, $p = 0.0067$) (**b**) at 24 h

Expression of PI3K/AKT and ERK1/2/MAPK by CM-hMSCA in Cells Subjected to *Scratch* Assay

In Fig. 3, we show that cells under *scratch* + BSS0 + CM2% increased AKT expression up to 135% (Fig. 3, A) and its phosphorylated form up to 102.8% in comparison to *scratch* + BSS0 (Fig. 3, B). Similar results were observed with the increase in ERK1/2 expression up to 134.7% (Fig. 3, C) and its phosphorylated form up to 55.4% against *scratch* + BSS0 (Fig. 3, D).

The Levels of Gene Expression Involved in the Processes of Mitochondrial Dynamics and Respiratory Chain Are Regulated by the CM-hMSCA in Cells Subjected to *Scratch*

Next, we evaluated the expression levels of *mnf1*, *mnf2*, *fis1*, *Drp1*, *opa1*, *ND1*, and *ND2* (Table 1, Fig. 4), all of them implicated in mitochondrial dynamics and functionality. In *scratch* + BSS0 cells, the expression of genes involved in mitochondrial fusion was regulated positively at 24 h: 54% *mnf1* (Fig. 4a) and 98% *mnf2* (Fig. 4b) and fission: 124% *fis1* (Fig. 4c) and 220% *Drp1* (Fig. 4d) compared to control (*scratch* + BSS5). In *scratch* + BSS0 + CM2% cells, expression of fission genes (*fis1* and *Drp1*) was negatively regulated around ≅ − 45% compared to the *scratch* + BSS0 group (Fig. 4c, d). Also, in *scratch* + BSS0 cells, we observed an increased gene expression of ND1 (46.1%, Fig. 4e) and ND2 (34%, Fig. 4f) in respect to control (*scratch* + BSS5), and decreased expression for *opa1* (− 54%, Fig. 4g). Upon treatment with CM2%, the expression of these genes was found reduced (− 44.1% -*opa1*, − 75.7% -ND1, and − 50.3% for ND2).

Mitochondrial Inhibition and Ngb Blockade Dampen the Protective Effect of CM-hMSCA in Cells Subjected to *Scratch* Assay

To determine whether mitochondria are an important mediator of the protective effects exerted by CM-hMSCA, we treated astrocytic cells with antimycin A (AA) (see "Mitochondrial Inhibition in Cell Culture"), a mitochondrial inhibitor, at different times (0–2–4–6–12–18–24 h) (Fig. 5). In cells exposed to *scratch* + BSS0 + AA, we observed a decrease in viability

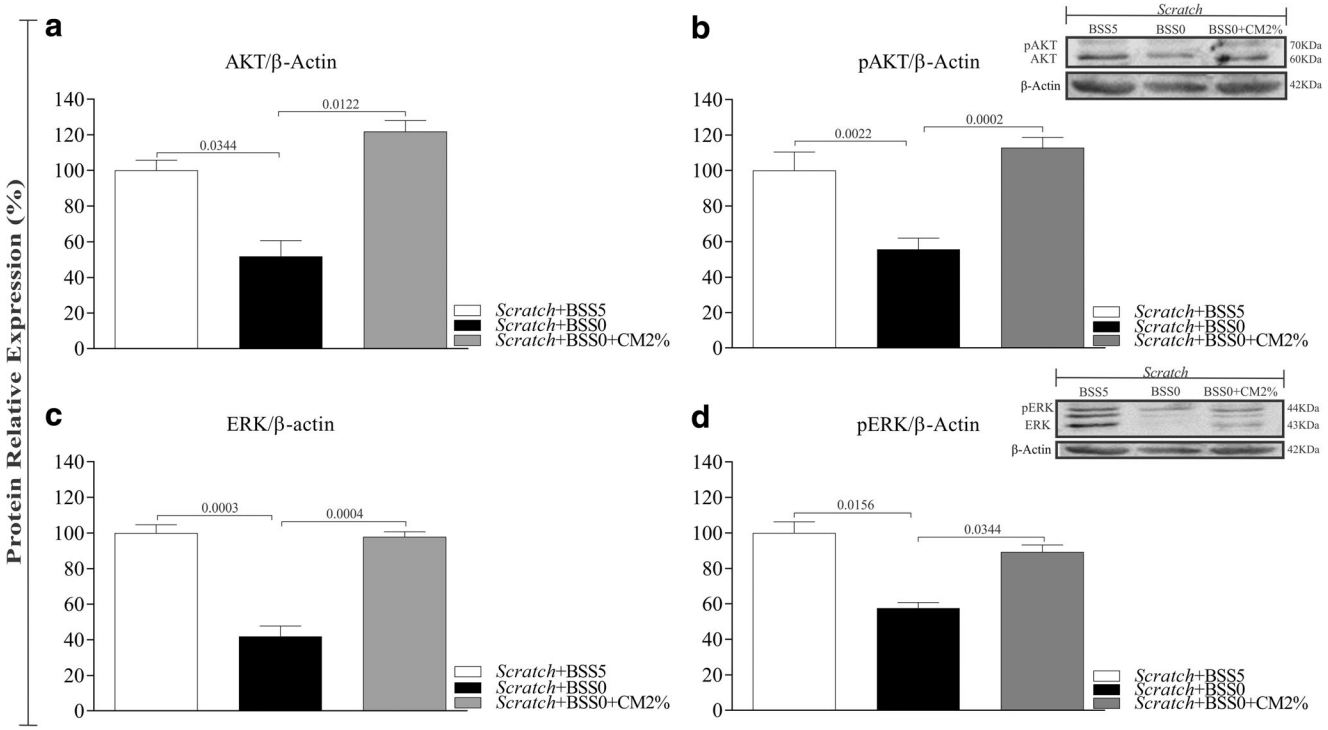

Fig. 3 Expression of PI3K/AKT and ERK1/2/MAPK by CM-hMSCA in cells under *scratch* + BSS0 and CM2%. The western blot analysis indicated that total AKT expression was higher in cells treated with 2% CM-hMSCA (*scratch* + BSS0 + CM2% vs. *scratch* + BSS0, $p = 0.0002$) (A) and AKT phosphorylation levels also increased significantly in *scratch* + BSS0 + CM2% vs. *scratch* + BSS0 cells ($p = 0.0001$) (B). Similarly, an increase in the levels of ERK1/2 ($p = 0.0001$) (C) and its phosphorylation ($p = 0.0081$) (D) was observed in *scratch* + BSS0 + CM2% vs. *scratch* + BSS0. β-Actin was used as charge control. All the data in these figures are presented as mean ± SEM of three individual experiments

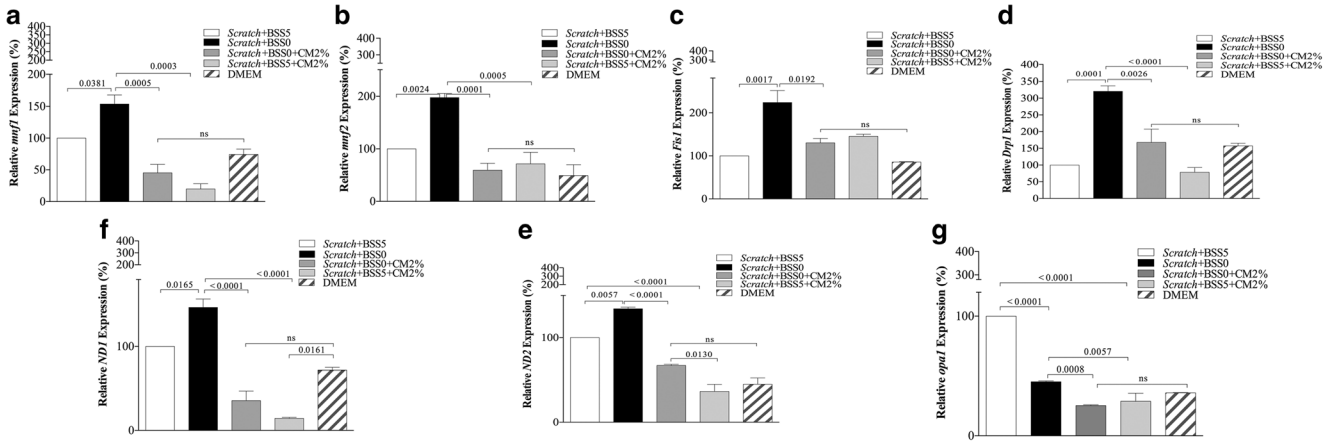

Fig. 4 Effect of CM-hMSCA on the mitochondrial dynamics and the respiratory chain of cells subjected to *scratch* assay. The specific quantification of the fusion genes, *mfn1* (**a**) and *mfn2* (**b**), and fission genes, *Fis1* (**c**) and *Drp1* (**d**), as well as ND1 (**e**), ND2 (**f**), and *opa1* (**g**) was performed by RT-PCR. In *scratch* + BSS0 cells, *mnf1* was positively regulated (*scratch* + BSS0 vs. *scratch* + BSS5, $p = 0.0381$, **a**) as well as *mnf2* (*scratch* + BSS0 vs. *scratch* + BSS5, $p = 0.0024$, **b**), as genes responsible for mitochondrial fusion. Similar results were observed with *fis1* (*scratch* + BSS0 vs. *scratch* + BSS5, $p = 0.0017$, **c**) and *Drp1* (*scratch* + BSS0 vs. *scratch* + BSS5, $p = 0.0001$, **d**), which in turn are involved in mitochondrial fission. Treatment with 2% of CM-hMSCA reduced the expression of these genes with respect to the *scratch* + BSS0 ($p = 0.0026$ –*Drp1*) ($p = 0.0192$ –*fis1*) ($p = 0.0005$ –*mnf1*) ($p = 0.0001$ – *mnf2*). Likewise, a significant decrease was found in *opa1* levels (*scratch* + BSS0 + CM2% vs. *scratch* + BSS0, $p = 0.0008$, **g**), ND1 (*scratch* + BSS0 + CM2% vs. *scratch* + BSS0, $p < 0.0001$, **e**), and ND2 (*scratch* + BSS0 + CM2% vs. *scratch* + BSS0, $p < 0.0001$, **f**) after 24 h. The data was normalized to GAPDH. The data represent the percentage of control expressed as means ± SEM of triplicates of three experiments

percentage from 78.4% at 2 h to 21.4% at 24 h (Fig. 5a). Likewise, cells treated with *scratch* + BSS0 + CM2% + AA showed reduced viability (by 86.4%) compared with cells exposed only to *scratch* + BSS0 + CM2% at 24 h. To verify whether treatment with AA inhibited the mitochondrial activity, we evaluated parameters related to mitochondrial function. Our results showed a decrease by 66% in ΔψM (Fig. 5b), and a reduction of up to 60.3% in the antioxidant protection of cardiolipin that is related to active and stable mitochondria assessed by Nonyl Acridine Orange (NAO) (data not shown). ROS production was increased respective to time up to 18.7% for O_2^- at 24 h (Fig. 5c) and a decrease in H_2O_2 by 30.5% (data not shown) at 24 h. During this assay, we observed that at 6 h most of the parameters determined had a different behavior than the other times. For this reason, in future tests, we took two time points at 6 h and 24 h.

Next, we explored whether the protective effect of CM-hMSCA was mediated by Ngb, as previously reported by our group showing that CM2% increases Ngb expression [10]. Ngb gene expression was silenced using RNA interference (RNAi) (Fig. 6, A). Blockade of Ngb was confirmed by western blotting (see "Protein Expression and Western Blotting") (Fig. 6, A). Since neuroglobin can migrate to mitochondria and interact with different proteins upon cell damage, we inhibited this organelle using AA (for 6 and 24 h) to investigate whether mitochondria are important for neuroglobin to exert protection in our model. We found that in cells exposed to *scratch* + BSS0 + CM2% + siRNA-Ngb + AA for 24 h, cell viability reached only 6.5% (Fig. 5d) while ΔψM was lost by up to 27.4% (Fig. 5e) and an increase of up to 103.1% in ROS production was observed (Fig. 5f).

Effect of Neuroglobin Blockade on the Expression of Proteins Involved in Cell Survival, Oxidative Stress, and Cellular Ca^{2+}

Figure 6 shows the confirmation of previous findings [10], whereby Ngb is involved in the protective actions of CM-hMSCA. To corroborate the role of Ngb in the protective effect of CM-hMSCA, we determined the expression of proteins related to different cell functions. Our results showed that silencing of Ngb significantly reduced the expression of AKT (52.8%) and ERK1/2 (27%), as well as the phosphorylated state of each protein (43.8% for pAKT, Fig. 6, B and C, and 70.8% for pERK1/2, Fig. 6, D and E) in *scratch* + BSS0 + CM2% + siRNA-Ngb cells in comparison to *scratch* + BSS0 + CM2%. In addition, blockade of Ngb protein in *scratch* + BSS0 + CM2% + siRNA-Ngb cells at 24 h reduced the expression of the antioxidant proteins superoxide dismutase (SOD2) (Fig. 6, F), catalase (Cat) (Fig. 6, G), and glutathione peroxidase (GPX1) (Fig. 6, H) by 80%, 43.6%, and 23%, respectively.

Blockade of Ngb also had an impact on cellular Ca^{2+} levels. Cells exposed to *scratch* + BSS0 + CM2% + siRNA-Ngb had a reduction by 10.7% in the level of $[Ca^{2+}]_{cyto}$ compared to *scratch* + BSS0 cells. However, no change was

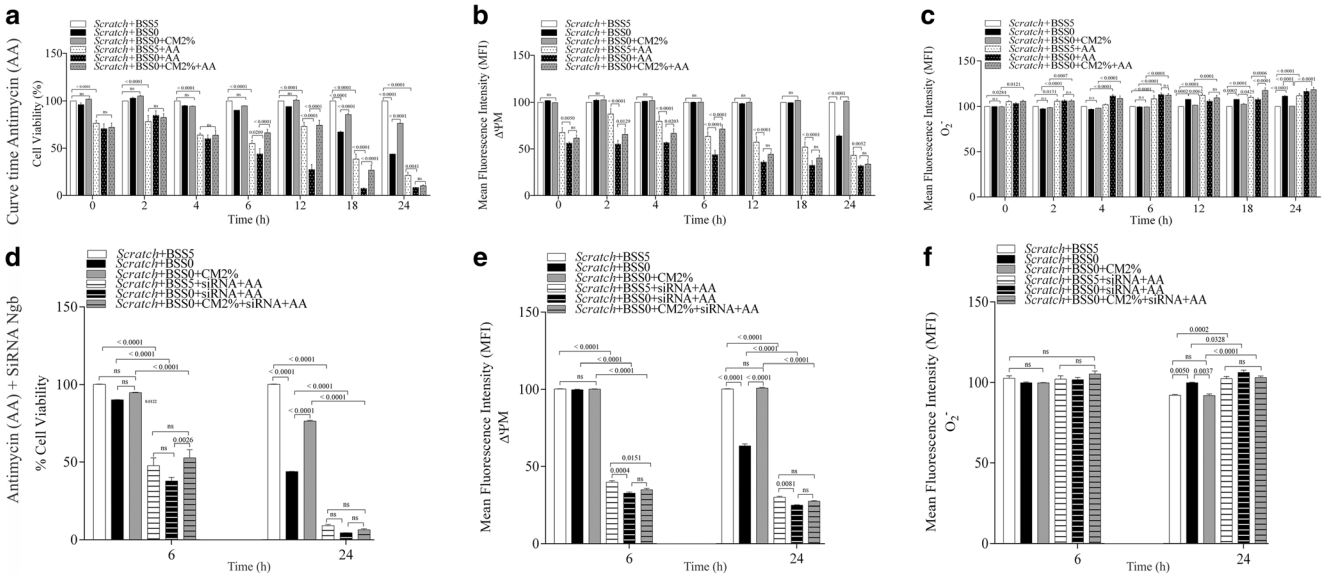

Fig. 5 Ngb and mitochondrial activity are mediating the protective effect of CM-hMSCA. The bar graph shows cells *scratch* + BSS0 + CM2% + AA vs. *scratch* + BSS0 + CM2%, in which the protective effect of CM-hMSCA was considerably reduced ($p < 0.0001$) at 24 h (**a**); likewise, there was a significant loss in ΔψM (*scratch* + BSS0 + CM2% + AA vs. *scratch* + BSS0 + CM2%, $p < 0.0001$, **b**) and an increase in ROS production (*scratch* + BSS0 + CM2% + AA vs. *scratch* + BSS0 + CM2%, $p < 0.0001$, **c**). Design bars (dots) are experimental groups in presence of AA. Also, in the bar graph, the siRNA-Ngb together with the AA inhibitor suppressed almost completely the protective effect of the CM-hMSCA in all parameters determined, such as viability (**d**), ΔψM (**e**), and ROS (**f**) in cells (*scratch* + BSS0 + CM2% + AA + siRNA-Ngb vs. *scratch* + BSS0 + CM2%, $p < 0.0001$, as well as for *scratch* + BSS5 + AA + siRNA-Ngb vs. *scratch* + BSS5, $p = 0.0002$). Design bars (horizontal lines) are experimental groups with siRNA-Ngb + AA

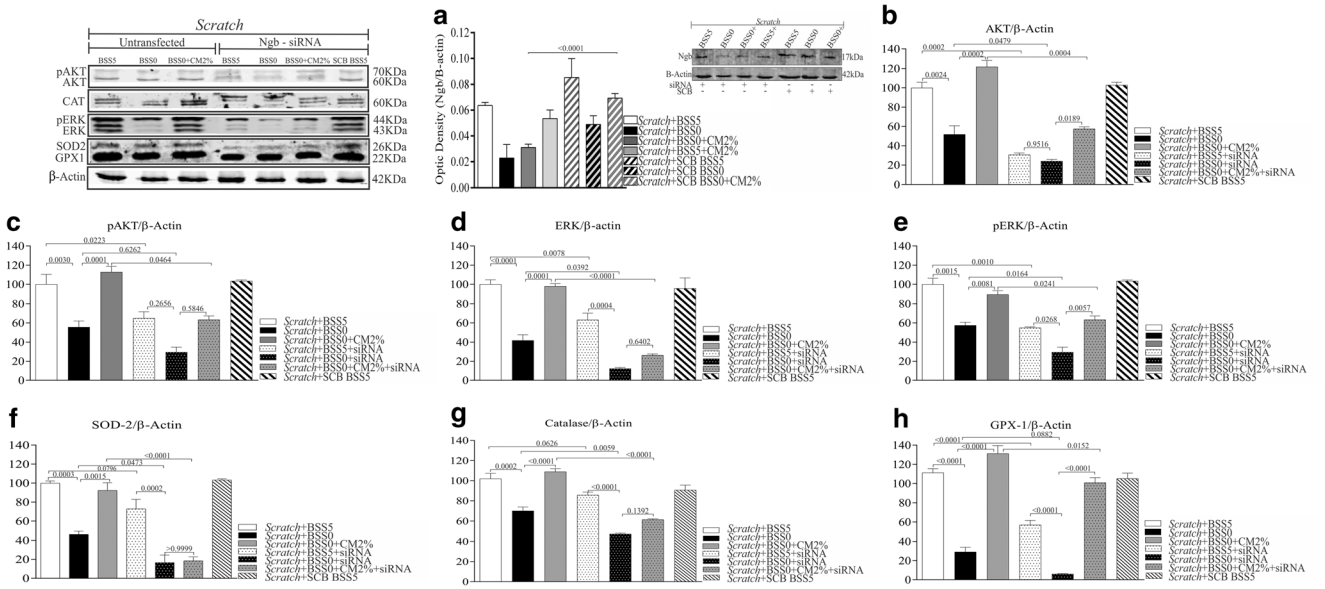

Fig. 6 Effect of neuroglobin silencing on protein expression, oxidative stress, and cellular Ca^{2+}. Validation of Ngb siRNA by western blotting. The silencing of Ngb significantly reduced Ngb levels in both cell groups *scratch* + BSS0 ($p < 0.0001$) and the control *scratch* + BSS5 ($p < 0.0001$) (A). The silencing of Ngb significantly reduced the expression of AKT ($p = 0.0004$, B), pAKT ($p = 0.0464$, C), ERK1/2 ($p < 0.0001$, D), and pERK ($p = 0.0241$, E) at 24 h, as well as affected the expression of antioxidant proteins such as SOD2 ($p < 0.0001$, F), catalase ($p < 0.0001$, G), and GPX1 ($p = 0.0152$, H) in cells exposed to *scratch* + BSS0 + CM2% + siRNA-Ngb vs. *scratch* + BSS0 + CM2%

observed either in cells exposed to *scratch* + BSS5 + siRNA-Ngb or in the group exposed to *scratch* + BSS0 + CM2% + siRNA-Ngb (Fig. S1-A). Interestingly, in cells exposed to *scratch* + BSS0 + siRNA-Ngb, the $[Ca^{2+}]_{mito}$ decreased significantly by 51.4% compared to that in *scratch* + BSS0 cells at 24 h. Similar results were observed for cells exposed to *scratch* + BSS0 + CM2% + siRNA-Ngb with a reduction of 57% in $[Ca^{2+}]_{mito}$ and a reduction of about 23.7% in cells exposed to *scratch* + BSS5 + siRNA-Ngb. These differences were obtained by comparing different experimental groups with and without siRNA (Fig. S1-B). Also, as for $[Ca^{2+}]_{ER}$ at 24 h, we observed a reduction close to 57% after *scratch* + BSS5 + siRNA-Ngb compared to cells without Ngb silencing (Fig. S1-C). However, although there was a decrease in $[Ca^{2+}]_{cyto}$ after Ngb silencing, this is still higher compared to $[Ca^{2+}]_{mito}$ and $[Ca^{2+}]_{ER}$.

Expression and Co-localization of Neuroglobin in Cellular Organelles Is Stimulated by CM-hMSCA in Cells Subjected to *Scratch* Assay

To determine whether the CM-hMSCA, in addition to positively regulating Ngb as reported in previous studies [10], could stimulate the subcellular localization of this protein in different compartments, an initial qualitative analysis was performed using fluorescence microscopy (Fig. 7). Analysis by fluorescence microscopy showed the co-localization of Ngb with Mito-RFP (Fig. 7, A), Golgi-RFP (Fig. 7, B), and ER-RFP (Fig. 7, C). Our results showed that in cells exposed to *scratch* + BSS0 + CM2%, the merged signals for Ngb-Mito-RFP were significantly increased by 27.8% (Fig. 7, D). On the contrary, we observed a reduction for the merged signals of Ngb-Golgi-RFP (43.4%) and Ngb-ER-RFP (30%) in cells exposed to *scratch* + BSS0 + CM2% compared with control (*scratch* + BSS5) cells. On the other hand, it should be noted that in *scratch* + BSS5 cells there was a 66% more merged signal in Ngb-ER-RFP and 90% in the case of Ngb-Golgi-RFP when compared with the *scratch* + BSS0 group (Fig. 7, D). It is noteworthy that the Ngb signal increased approximately 2.9 times more in the mitochondrial compartment of cells treated with *scratch* + BSS0 + CM2% compared with *scratch* + BSS0 (Fig. 7, D).

Discussion

A large number of brain pathologies involve an inflammatory component that significantly affects brain function [52–54]. Astrocytes are specialized cells with multiple functions [55–57] within the CNS and are able to regulate or influence neuroinflammation [58, 59], depending on the state of involvement and duration of the injury. In this regard, the fact that astrocytes regulate inflammation and prevent the progression of the injury has prompted strategies aimed to preserve their functions and thus promote neuronal survival upon any pathological event including TBI. A previous work from our laboratory showed that CM-hMSCA exerts neuroprotective effects on astrocytes under *scratch* injury. In the present work, we aimed to determine possible mechanisms of action of CM-hMSCA in astrocytes using the same in vitro model. Our

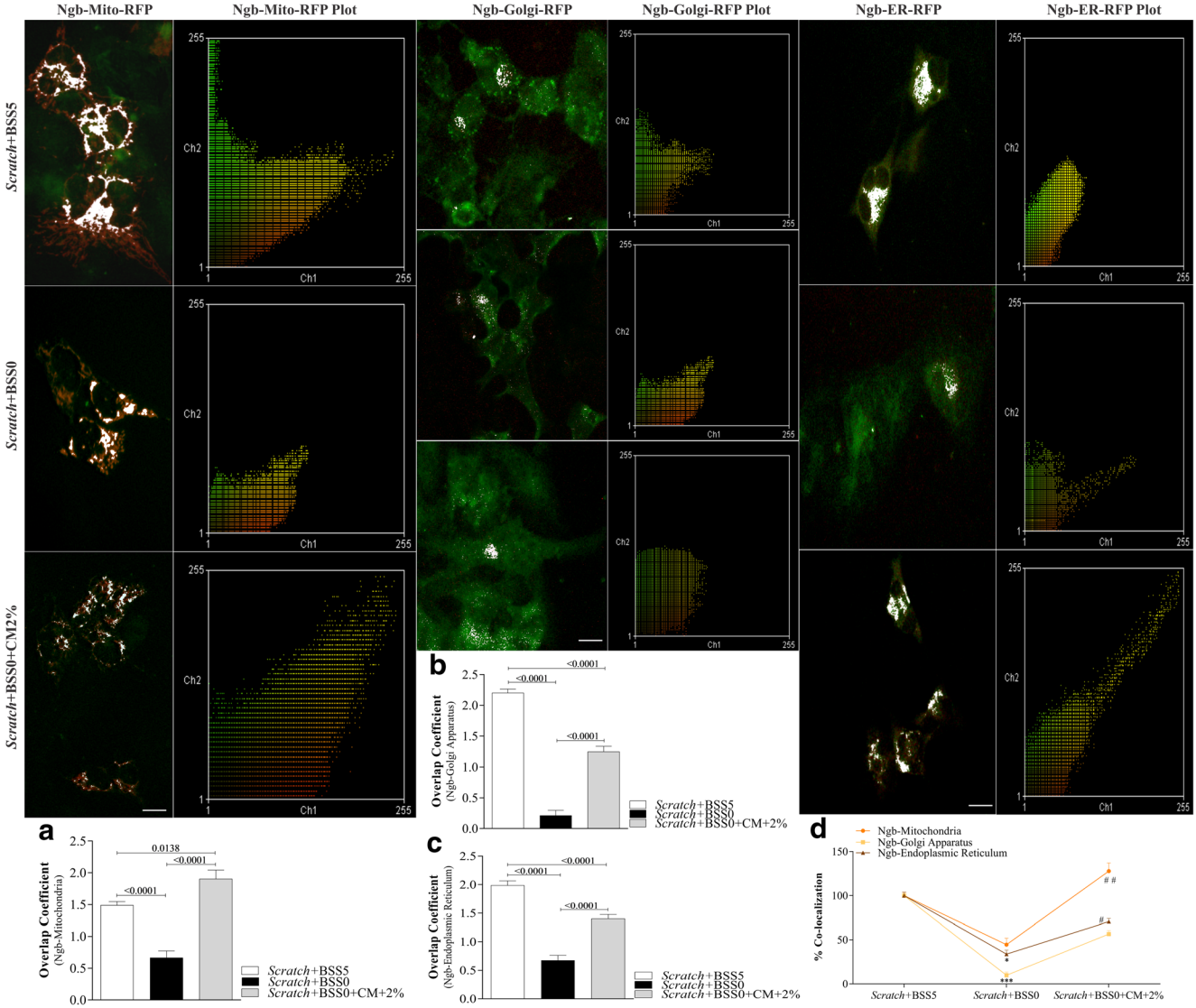

Fig. 7 Expression and co-localization of Ngb in different subcellular compartments. The top panel shows merged images of the expression of Ngb (green) in different organelles (red) for three representative experimental groups. The percentage of positive cells was obtained by separate analysis of each marker, that is, Ngb, mitochondria (Mito-RFP) (microphotographs and plots in left panel; A), in Golgi apparatus (Golgi-RFP) (microphotographs and plots in central panel; B), and in endoplasmic reticulum (ER-RFP) (microphotographs and plots in right panel; C). The areas calculated by the Intensity Correlation Analysis plugin of the ImageJ software are shown in white points. Each scatter diagram represents the correlation between the green and red frequencies of the cells; the yellow area of the scatter plot accounts for the co-localization of the staining, that is, the organelles (red) and the neuroglobin (green). The results of the analysis are plotted as a percentage of co-localization between organelles and Ngb. Ngb and Mito-RFP showed a significant co-localization in cells exposed to *scratch* + BSS0 + CM2% vs. *scratch* + BSS0 ($p < 0.0001$, A) and even between cells exposed to *scratch* + BSS0 + CM2% vs. *scratch* + BSS0 ($p = 0{,}0138$, A). Three asterisks, significant differences, Ngb-Golgi apparatus vs. Ngb-mitochondria for cells exposed to *scratch* + BSS0 ($p = 0.0008$) (D). One asterisk, significant differences, Ngb-endoplasmic reticulum vs. Ngb-Golgi apparatus for cells exposed to *scratch* + BSS0 ($p = 0.0232$) (D). Two number signs, Ngb-Golgi apparatus vs. Ngb-mitochondria ($p < 0.0001$) (D). One number sign, Ngb-endoplasmic reticulum vs. Ngb-mitochondria for cells exposed to *scratch* + BSS0 + CM + 2% ($p < 0.0001$) (D). Scale 20 μm

results showed that CM-hMSCA regulates the cytokines IL-2, IL-6, IL-8, IL-10, GM-CSF, and TNF-α, and regulates Ca^{2+} at the cytoplasmic level. These results were accompanied by the regulation of mitochondrial dynamics and genes (*opa1*, *mnf1* and *mnf2*, *fis1*, *Drp1*), as well as induced expression of survival cascades such as AKT/pAKT and ERK1/2/pERK. Indeed, we observed that CM-hMSCA regulates the subcellular localization of Ngb and that blockade of this protein affects Ca^{2+} dynamics and mitochondrial functions.

During CNS damage, there should be a homeostatic balance between an optimal antioxidant response and inflammatory event. A physiological balance between anti- and pro-inflammatory molecules is essential for proper neuroprotective response to any insult or injury that affects brain tissue.

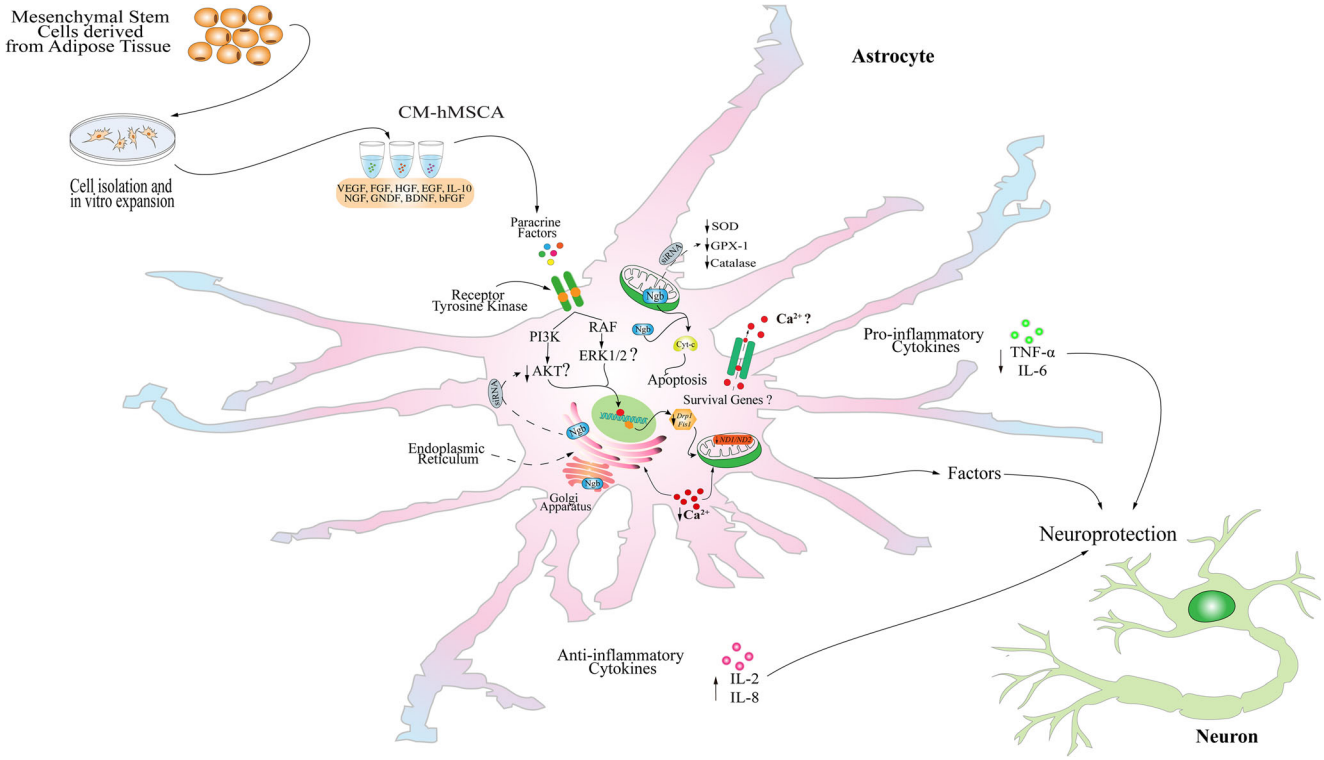

Fig. 8 Proposal mechanisms of the effect of 2% of CM-hMSCA in the protection of our astrocytic model (T98G) exposed to *scratch* assay. A mechanical injury associated with metabolic alterations is associated with cell damage through the increase in ROS generation, alteration of cellular signaling pathways, mitochondrial dynamics, and intracellular Ca^{2+} levels that lead to cell loss and deterioration of cognitive and motor functions. In this study, we observed that 2% of CM-hMSCA during 24 h has an effect on the secretion of cytokines, in the regulation of Ca^{2+} and mitochondrial dynamics, possibly mediated by an interaction of Ngb and mitochondria. Altogether, CM-hMSCA induces the expression of AKT and ERK1/2 and antioxidant proteins, thus regulating in part the inflammatory and apoptotic processes and maintaining astrocytes functions

However, during TBI, the brain cells (namely astrocytes and microglia) secrete cytokines and mediators such as IL-1, TNF-α, IL-12, IFNγ, IL-6, prostaglandins, and nitric oxide, among other molecules that are positively regulated, thereby causing neuronal death [58, 60, 61]. This information is in agreement with our findings, in which an increase of the cytokines IL-6, TNF-α, and GM-CSF was observed after 24 h in astrocytic cells subjected to *scratch* + BSS0 (Fig. 1). Nevertheless, we found a decrease in the levels of these cytokines in *scratch* + BSS0 + CM2% after 24 h (Fig. 1). This can be explained by the fact that MSC secretion includes growth factors, chemokines, cytokines, and extracellular vesicles [62] in addition to the immunomodulatory ability of adipose-derived mesenchymal stem cells (AMSC) [12, 63–65]. Likewise, previous studies reported a clear relationship between a traumatic injury of human astrocytes in an in vitro model and positive regulation of IL-6 which induces astrogliosis and angiogenesis, both necessary for tissue remodeling and recovery [66]. However, sustained IL-6 expression is related to the pathogenesis of neurodegenerative diseases, astrogliosis [67, 68], and experimental autoimmune encephalomyelitis (EAE) [69]. Therefore, the search for alternatives to decrease or regulate IL-6 and other cytokines may be promising for the recovery of brain tissue. Surprisingly, in this study, a significant decrease in TNF-α in *scratch* + BSS0 + CM2% was observed (Fig. 1), which is remarkable considering that low levels of TNF-α are important for brain tissue recovery [70]. We also observed that the level of IL-6 in cells exposed to *scratch* + BSS0 + CM2% remained similar to that of the control (*scratch* + BSS5) (Fig. 1). This finding supports the idea that maintaining basal levels of IL-6 has benefits in increased CNS wound healing after traumatic injury [71, 72] and in the regulation of glial activation [73–76]. Besides, it is known that IL-6 is regulated by other cytokines like TNF-α or IL-1β [77]. Interestingly, IL-6 was found to be responsible for an increase in ATP levels that may be related to the recovery of mitochondrial ultrastructure, and is also involved in improving mitochondrial biogenesis and autophagy in an astrocytic model of experimental sepsis [78]. These findings can explain, at least in part, the protective effects of CM-hMSC at the mitochondrial level [9, 10]. However, more studies are necessary to clarify the mechanisms of protection.

In this study, we found that IL-2 and IL-8 were elevated in *scratch* + BSS0 + CM2% cells at 24 h (Fig. 1). These cytokines are considered to have neuroprotective functions. For example, IL-2 can stimulate proliferation and promote

survival and neurite extension of cultured neurons [79] and the processes of myelination and differentiation of oligodendrocytes [80]. Likewise, IL-2 can regulate inflammation through the Treg cells [81]. Similar results were obtained with IL-8, also known as CXCL8 [82]. This cytokine also showed an increase in astrocytes in the *scratch* + BSS0 + CM2% after 24 h (Fig. 1). This is interesting because IL-8 can apparently regulate inflammation at the level of nervous tissue [68, 82–84], besides mediating angiogenic functions [68] and neuroprotection through the activation of CXCR2 [85] or anti-apoptotic proteins such as Bcl-2 and Bcl-X1 [86].

We also examined IL-10 which is considered as an anti-inflammatory and neuroprotective mediator [80, 87, 88]. However, we did not observe any alteration in this cytokine in the *scratch* + BSS0 + CM2% group, which can be explained by the presence of IL-10 in CM-hMSCA, as well as other molecules with protective effect in brain tissue [84, 89–94]. Although many cytokines have benefits within the CNS, the complete profile of cytokines and chemokines derived from astrocytes during inflammation is not yet fully characterized. CM-hMSCA regulates some cytokines, and these molecules are responsible for mediating not only the inflammatory processes, but also calcium channels, brain excitability, and synapse formation [95–97]. We also investigated the changes of Ca^{2+} in the cytosol, the mitochondria, and the endoplasmic reticulum. We found that cells subjected to *scratch* + BSS0 showed a significant increase in cytoplasmic calcium at 24 h (Fig. 2a). This observation can be explained by the fact that both glial cells and neurons respond to OGD with reversible membrane depolarizations that sustainably increase intracellular Ca^{2+} [98, 99]. Interestingly, in the group of cells treated with *scratch* + BSS0 + CM2%, we observed a significant reduction of cytoplasmic calcium at 24 h (Fig. 2a), which may be related to the mediation of trophic factors such as FGF, BDNF, EGF, and NGF that are present in CM-hMSC and can provide neuroprotection [84, 89–92, 100, 101], or the presence of molecules such as TNF that can serve as a protective mediator in the CNS [102]. TNF has been recognized in several studies as a neuronal protector [103–105] that can attenuate elevation of stimulus-induced intracellular Ca^{2+} [105].

It is well known that the signaling and homeostasis of Ca^{2+} are not only at the cytoplasmic level, but also other compartments such as mitochondria and ER are responsible for regulating this ion and its signaling inside the cells [106, 107]. In the present study, we found that the decrease in Ca^{2+} in the intracellular space in cells under *scratch* + BSS0 + CM2% (Fig. 2a) was related to a distribution of this ion to other organelles such as mitochondria (Fig. 2b) and, though not significantly, ER (Fig. 2c) at 24 h. This is somehow interesting given that the ER is directly involved in Ca^{2+} signaling [108]. Depletion of Ca^{2+} in the ER not only prevents the triggering of an ER stress response (ERSR) [108], but also contributes to a delay in the elevation of intracellular Ca^{2+} [109]. On the other hand, we also observed a Ca^{2+} influx to mitochondria in cells subjected to *scratch* + BSS0 + CM2% at 24 h (Fig. 2b). This slight increase in mitochondrial Ca^{2+} can be explained by the fact that a mitochondrion is another organelle responsible for the regulation of Ca^{2+} in glial cells [107, 110, 111] and there is a permanent crosstalk between this organelle and the ER [110]. Indeed, mitochondria can act as a buffer through which cytosolic overloads of Ca^{2+} are regulated [107, 112]. The effects of CM-hMSCA on the regulation of Ca^{2+} could be explained by the presence of several molecules including EGFP [113] and bFGF [114], both implicated in mediating Ca^{2+} responses through the regulation and function of the glutamate receptor in neurons or any of the AMPA receptor subunits [102, 114]. However, all these investigations have been carried out in neurons, with a lack of studies on astrocytes. For this reason, it is essential to expand and develop more in-depth research in relation to this topic.

With the regulation of calcium in cell organelles, it is likely that CM-hMSCA not only preserves the ultrastructure, but also may regulate the processes of mitochondrial dynamics [10]. To go further, we assessed genes related to mitochondrial dynamics and oxidative phosphorylation in cells exposed to *scratch* assay and/or CM2%. Our results demonstrated a downregulation of *mfn1* and *mfn2* genes (Fig. 4a, b), which are responsible for mitochondrial fusion [115, 116], and *fis1* (Fig. 3, C), which is directly responsible for mitochondrial fission (reviewed by [117–119]). Surprisingly, these genes were upregulated in cells under *scratch* + BSS0, suggesting fusion-fission processes are deregulated in these cells. Nevertheless, upon treatment with CM2%, the expression of these fusion-fission genes is diminished, suggesting that possible factors present in the conditioned medium might contribute in part to maintain mitochondrial dynamics. Homeostasis in mitochondrial dynamics is key for cellular functions in general, not only from the metabolic point of view, but also it is indispensable to prevent deregulation of Ca^{2+} or mitochondrial signaling leading to abnormal function and even death [120, 121] and cellular stress [122–124]. Interestingly, when evaluating other genes implicated in mitochondrial function (*Drp1* and *opa1*), our results showed a positive regulation in the expression of *Drp1* and *opa1* in cells under *scratch* + BSS0 but, surprisingly, a significant decrease in cells exposed to CM2% (*scratch* + BSS0 + CM2%, Fig. 3, D–G). For instance, these genes (*Drp1* and *opa1*) are associated to mitochondrial dynamics, including cellular apoptosis [125–127]. Different studies have suggested that *Drp1* plays an important role in fission [127, 128], mitochondrial fragmentation, and apoptosis-like cell death [125–127]. These results suggest that CM-hMSCA may regulate the mitochondrial dynamics in astrocytic cells subjected to *scratch* + BSS0. In this study, we found a decrease in the expression of *Drp1* and *fis1*, both genes being responsible for mitochondrial fission

[118, 129] in cells subjected to *scratch* + BSS0 + CM2%. This finding is supported by several studies [118, 130–133], in which a blockade of *Drp1* and negative regulation of *fis1* protected the cells from apoptosis by decreasing the release of cytochrome c.

Cells subjected to *scratch* + BSS0 + CM2% presented less *opa1* levels (Fig. 3, G), a result that we did not expect taking into account that *opa1* is related to different mitochondrial functions [134, 135] and the control of apoptosis [134, 136]. This suggests that cells under *scratch* + BSS0 + CM2% may develop a mechanism different from *opa1* for their survival, possibly related to autophagy. In relation to the latter, it is known that autophagy is a process mediated by oxidative stress, nutrient deprivation, and cell damage, among others [137], associated with quality control and survival [138–140]. In this regard, previous research carried out by our group showed that cells subjected to *scratch* + BSS0 + CM2% had larger mitochondria and a higher number of ridges, which are correlated to previous studies showing that low levels of *opa1* are related to autophagy processes [141, 142]. Likewise, it has been reported that during autophagy, mitochondria lengthen, spared from degradation and maintain cellular viability [130], apparently maintaining a higher number of ridges through which ATP production is optimized during nutrient restriction [143, 144] or simply *opa1* may be directly involved in the integration of the cellular metabolic state [145, 146]. We found the same pattern with two other genes *ND1* and *ND2*, two subunits of complex I. This is important not only because complex I is involved in disease states for contributing to the production of ROS and the decrease in energy, but also because it is being evaluated as a possible therapeutic alternative for encephalomyopathies and neurodegenerative diseases [147–149]. In the present study, we found that both *ND1* and *ND2* were positively regulated in *scratch* + BSS0 cells and, surprisingly, their expression was attenuated when *scratch* cells were treated with CM2% (Fig. 3, E and F). These findings may be related to previously reported results, in which CM-hMSCA significantly decreased ROS production [10, 18] and oxidative damage possibly through overexpression of antioxidant or mediator proteins such as neuroglobin (Ngb) [10] or the binding of Ngb to subunits of mitochondrial complexes [150]. Despite these findings, the molecular mechanisms that can regulate the fusion processes or the action on the respiratory chain are still not clear, and it is not known if the trophic factors, neurotrophic factors, and anti-apoptotic and anti-inflammatory molecules of CM-hMSCA can directly mediate these processes within the cell. Likewise, and supporting in part the previous findings, in this study, we showed that CM-hMSCA exerts its effect through the protection of the mitochondria. Our results showed that upon inhibition of mitochondria with AA (Fig. 5), the protective effect of CM-hMSCA in *scratch* + BSS0 + CM2% cells was abolished. These damaging effects reduced cell viability (Fig. 5a), augmented both ROS production (Fig. 5b) and $\Delta\psi M$ loss (Fig. 5c). Indeed, this protective action of CM-hMSCA on scratched cells was completely dampened by inhibiting both mitochondria and genetic silencing of Ngb (Fig. 5d–f). These findings suggest that 2% CM-hMSCA can favor astrocyte protection through preservation of mitochondrial functioning and the action of Ngb in neutralizing ROS or inhibiting apoptosis through a mitochondrial-dependent pathway [23–26, 151].

In a preliminary attempt to determine the mechanism of action of the CM-hMSCA, we investigated whether CM-hMSCA may regulate the expression of biologically important proteins involved in signaling pathways. We showed that *scratch* + BSS0 + CM2% cells increased AKT phosphorylation and possible expression of the PI3K/AKT signaling (Fig. 3, A and B) and similar results were observed with ERK1/2 and pERK (Fig. 3, C and D), both being important in cell survival [21, 152–154]. This finding suggests that CM-hMSCA may probably activate survival mechanisms against *scratch* + BSS0 damage mediated by PI3K/AKT, ERK1/2/MAPK, or both. These pathways are quite known to be activated by growth factors [155–158], which are all present in MSc's secretome [92, 152, 159]. In these studies, many biological factors have been found including VEGF, βFGF, PDGF, IGF-1, and S1P, all of which have anti-apoptotic activity and the ability to upregulate the mostly anti-inflammatory factors TGFβ1 and IL-1 [24, 160, 161]. Indeed, this study also assessed the expression of the AKT and ERK1/2 pathways in the *scratch* + BSS0 model. The increase in phosphorylation and expression of these proteins may not only mediate the survival of astrocytes in conditions of *scratch* + BSS0, but also supports the protective effects of CM-hMSCA possibly through the PI3K/AKT or ERK1/2/MAPK pathway or both. In this study, we also found that blockade of Ngb decreased the expression of phosphorylated proteins such as AKT (Fig. 6, B and C) and ERK1/2 (Fig. 6, D and E), as well as the antioxidant proteins SOD2 (Fig. 6, F), catalase (Fig. 6, G), and GPX1 (Fig. 6, H). It has been suggested that Ngb in astrocytes can influence oxygen homeostasis and protection against hydrogen peroxide through the activation of AKT, and prevent the activation of caspase 3 [23, 24]. Therefore, it is possible that CM-hMSCA-induced cytoprotection may be the result of Ngb activation by some factors present in CM-hMSCA or, simply, a secondary effect or action by activating signaling pathways such as PI3K/AKT or ERK1/2/MAPK or both, which in turn will upregulate antioxidant proteins such as those assessed in our study [9, 10, 18, 154, 162]. We also reported that siRNA-Ngb caused an imbalance in the movement of $[Ca^{2+}]_{cyto}$, $[Ca^{2+}]_{mito}$, and $[Ca^{2+}]_{ER}$ and interestingly these findings are supported by experimental studies that reported high levels of cytosolic Ngb suppressed Ca^{2+} levels and prevented the loss of ATP and $\Delta\Psi m$ normally associated with the onset of apoptosis

[163, 164] (Fig. 1S). Since the beneficial effects of the CM-hMSCA were significantly lost after adding siRNA-Ngb along with the blockade of mitochondria with AA (Fig. 5a–f), our results suggest that the protective effect of CM-hMSCA is mediated by the interaction of Ngb with mitochondria that affects the mitochondrial mechanisms of neuroprotection [26, 165–168]. In this way, with the findings obtained so far, we believe that Ngb remains an important protein to be considered as a mediator in the protection of CM-hMSCA in *scratch* + BSS0 cells. This is an important finding because therapeutic alternatives that promote the protection of mitochondria, especially astrocyte mitochondria, have become a major goal in neuroscience. It is noteworthy that in previous studies reported by us, the cells subjected to *scratch* + BSS0 + CM2% upregulated Ngb [10].

Due to the effects described in this, as well as other studies, Ngb is an attractive treatment target for pathologies such as TBI, ischemia, and even spinal cord injury since this protein is expressed in astrocytes and overexpressed in neurons of models established for the study of these pathologies [22–26]. However, it is not entirely clear if the location of the Ngb in the cells under *scratch* + BSS0 and *scratch* + BSS0 + CM2% is strictly mitochondrial or if it is present in other organelles. Moreover, it remains to be clarified if the location of Ngb depends strictly on the state of injury. Interestingly, our results showed an increased mitochondrial accumulation of Ngb (Fig. 7, A–D), followed by lower concentrations in other organelles such as the Golgi apparatus (Fig. 7, B) and the ER (Fig. 7, C). The data observed in the mitochondria in this study are consistent with previous reports [26, 165–167]. It is possible that some molecules that make up the secretome of hMSCs can interact with Ngb to produce a protective response in brain tissue. PDGF-BB [169], VEGF [170], and EPO [171] are some examples of these molecules. However, to our knowledge, this is the first study that addresses the presence Ngb in organelles other than mitochondria.

In conclusion, our results demonstrated the protective effects of CM-hMSCA in our astrocytic model against loss of viability and damage by oxidative stress induced by *scratch* + BSS0. This protective effect is possibly explained by the regulation of cytokines involved in inflammatory processes, as well as the mobilization of Ca^{2+} and its distribution within the intracellular compartments, thus avoiding a cytosolic fluctuation that triggers apoptotic pathways. CM-hMSCA increased PI3K/AKT and ERK1/2/MAPK, and modulated the expression of the genes responsible for mitochondrial dynamics. CM-hMSCA also regulated the expression of other protective proteins such as Ngb and its distribution within different organelles, from where it can exert different functions or mediate the expression of other proteins with antioxidant or survival functions in our *scratch* + BSS0 model (Fig. 8). In spite of the advances made so far, more experiments are still needed, such as starting to specifically determine the factors or molecules present in the CM-hMSCA that are beneficial for survival. It is also worth exploring if the protective effect is a synergy of all of the compounds present in the CM-hMSCA, as well as the mechanism of the molecules downstream of the PI3K/AKT and ERK1/2/MAPK pathways to promote cell survival and protection. In addition, understanding the mechanism of action of Ngb could provide a fundamental basis for the design of new pharmacological targets that suppress or prevent the death of astrocytes. The results of this study are beneficial to expand the understanding of the neuroprotective effects CM-hMSCA, even with a concentration of 2% as a treatment. Our findings confirm that CM-hMSCA has a beneficial effect on the survival and protection of CNS cells involved in various brain pathologies, suggesting a direct effect on astrocytes.

Acknowledgments The authors thank Dr. Jorge Andrés Afanador and the staff of the cosmetic surgery Clinic DHARA in Bogotá, Colombia, for the adipose tissue samples. This work was supported in part by grants PUJ IDs 6260 and 7115 to GEB and 6278 to JG and scholarship for doctoral studies awarded by the Vicerrectoría Académica of PUJ to EB.

Compliance with Ethical Standards

Conflict of Interest The authors declare that they have no conflict of interest.

References

1. Chen WW, Zhang X, Huang WJ (2016) Role of neuroinflammation in neurodegenerative diseases (review). Mol Med Rep 13(4): 3391–3396. https://doi.org/10.3892/mmr.2016.4948
2. Gonzalez H, Elgueta D, Montoya A, Pacheco R (2014) Neuroimmune regulation of microglial activity involved in neuroinflammation and neurodegenerative diseases. J Neuroimmunol 274(1–2):1–13. https://doi.org/10.1016/j.jneuroim.2014.07.012
3. Villegas-Llerena C, Phillips A, Garcia-Reitboeck P, Hardy J, Pocock JM (2016) Microglial genes regulating neuroinflammation in the progression of Alzheimer's disease. Curr Opin Neurobiol 36:74–81. https://doi.org/10.1016/j.conb.2015.10.004
4. Karve IP, Taylor JM, Crack PJ (2016) The contribution of astrocytes and microglia to traumatic brain injury. Br J Pharmacol 173(4):692–702. https://doi.org/10.1111/bph.13125
5. Sochocka M, Diniz BS, Leszek J (2017) Inflammatory response in the CNS: friend or foe? Mol Neurobiol 54(10):8071–8089. https://doi.org/10.1007/s12035-016-0297-1
6. Pedraza-Alva G, Perez-Martinez L, Valdez-Hernandez L, Meza-Sosa KF, Ando-Kuri M (2015) Negative regulation of the inflammasome: keeping inflammation under control. Immunol Rev 265(1):231–257. https://doi.org/10.1111/imr.12294
7. Ulusoy C, Zibandeh N, Yildirim S, Trakas N, Zisimopoulou P, Kucukerden M, Tasli H, Tzartos S et al (2015) Dental follicle mesenchymal stem cell administration ameliorates muscle weakness in MuSK-immunized mice. J Neuroinflammation 12:231. https://doi.org/10.1186/s12974-015-0451-0

8. Trubiani O, Giacoppo S, Ballerini P, Diomede F, Piattelli A, Bramanti P, Mazzon E (2016) Alternative source of stem cells derived from human periodontal ligament: a new treatment for experimental autoimmune encephalomyelitis. Stem Cell Res Ther 7:1. https://doi.org/10.1186/s13287-015-0253-4
9. Baez-Jurado E, Hidalgo-Lanussa O, Guio-Vega G, Ashraf GM, Echeverria V, Aliev G, Barreto GE (2018) Conditioned medium of human adipose mesenchymal stem cells increases wound closure and protects human astrocytes following scratch assay in vitro. Mol Neurobiol 55(6):5377–5392. https://doi.org/10.1007/s12035-017-0771-4
10. Baez-Jurado E, Vega GG, Aliev G, Tarasov VV, Esquinas P, Echeverria V, Barreto GE (2018) Blockade of neuroglobin reduces protection of conditioned medium from human mesenchymal stem cells in human astrocyte model (T98G) under a scratch assay. Mol Neurobiol 55(3):2285–2300. https://doi.org/10.1007/s12035-017-0481-y
11. Konala VB, Mamidi MK, Bhonde R, Das AK, Pochampally R, Pal R (2016) The current landscape of the mesenchymal stromal cell secretome: a new paradigm for cell-free regeneration. Cytotherapy 18(1):13–24. https://doi.org/10.1016/j.jcyt.2015.10.008
12. Guillen MI, Platas J, Perez Del Caz MD, Mirabet V, Alcaraz MJ (2018) Paracrine anti-inflammatory effects of adipose tissue-derived mesenchymal stem cells in human monocytes. Front Physiol 9:661. https://doi.org/10.3389/fphys.2018.00661
13. Guo ZY, Sun X, Xu XL, Zhao Q, Peng J, Wang Y (2015) Human umbilical cord mesenchymal stem cells promote peripheral nerve repair via paracrine mechanisms. Neural Regen Res 10(4):651–658. https://doi.org/10.4103/1673-5374.155442
14. Mita T, Furukawa-Hibi Y, Takeuchi H, Hattori H, Yamada K, Hibi H, Ueda M, Yamamoto A (2015) Conditioned medium from the stem cells of human dental pulp improves cognitive function in a mouse model of Alzheimer's disease. Behav Brain Res 293:189–197. https://doi.org/10.1016/j.bbr.2015.07.043
15. Pischiutta F, Brunelli L, Romele P, Silini A, Sammali E, Paracchini L, Marchini S, Talamini L et al (2016) Protection of brain injury by amniotic mesenchymal stromal cell-secreted metabolites. Crit Care Med 44(11):e1118–e1131. https://doi.org/10.1097/CCM.0000000000001864
16. Mekhemar MK, Adam-Klages S, Kabelitz D, Dorfer CE, Fawzy El-Sayed KM (2018) TLR-induced immunomodulatory cytokine expression by human gingival stem/progenitor cells. Cell Immunol 326:60–67. https://doi.org/10.1016/j.cellimm.2017.01.007
17. Fawzy El-Sayed KM, Dorfer CE (2016) Gingival mesenchymal stem/progenitor cells: a unique tissue engineering gem. Stem Cells Int 2016:7154327–7154316. https://doi.org/10.1155/2016/7154327
18. Torrente D, Avila MF, Cabezas R, Morales L, Gonzalez J, Samudio I, Barreto GE (2014) Paracrine factors of human mesenchymal stem cells increase wound closure and reduce reactive oxygen species production in a traumatic brain injury in vitro model. Hum Exp Toxicol 33(7):673–684. https://doi.org/10.1177/0960327113509659
19. Song M, Jue SS, Cho YA, Kim EC (2015) Comparison of the effects of human dental pulp stem cells and human bone marrow-derived mesenchymal stem cells on ischemic human astrocytes in vitro. J Neurosci Res 93(6):973–983. https://doi.org/10.1002/jnr.23569
20. Huang W, Lv B, Zeng H, Shi D, Liu Y, Chen F, Li F, Liu X et al (2015) Paracrine factors secreted by MSCs promote astrocyte survival associated with GFAP downregulation after ischemic stroke via p38 MAPK and JNK. J Cell Physiol 230(10):2461–2475. https://doi.org/10.1002/jcp.24981
21. Sun H, Benardais K, Stanslowsky N, Thau-Habermann N, Hensel N, Huang D, Claus P, Dengler R et al (2013) Therapeutic potential of mesenchymal stromal cells and MSC conditioned medium in amyotrophic lateral sclerosis (ALS)—in vitro evidence from primary motor neuron cultures, NSC-34 cells, astrocytes and microglia. PLoS One 8(9):e72926. https://doi.org/10.1371/journal.pone.0072926
22. Baez E, Echeverria V, Cabezas R, Avila-Rodriguez M, Garcia-Segura LM, Barreto GE (2016) Protection by neuroglobin expression in brain pathologies. Front Neurol 7:146. https://doi.org/10.3389/fneur.2016.00146
23. Amri F, Ghouili I, Amri M, Carrier A, Masmoudi-Kouki O (2017) Neuroglobin protects astroglial cells from hydrogen peroxide-induced oxidative stress and apoptotic cell death. J Neurochem 140(1):151–169. https://doi.org/10.1111/jnc.13876
24. Chen YX, Zeng ZC, Sun J, Zeng HY, Huang Y, Zhang ZY (2015) Mesenchymal stem cell-conditioned medium prevents radiation-induced liver injury by inhibiting inflammation and protecting sinusoidal endothelial cells. J Radiat Res 56(4):700–708. https://doi.org/10.1093/jrr/rrv026
25. Yu Z, Poppe JL, Wang X (2013) Mitochondrial mechanisms of neuroglobin's neuroprotection. Oxidative Med Cell Longev 2013:756989. https://doi.org/10.1155/2013/756989
26. Lan WB, Lin JH, Chen XW, Wu CY, Zhong GX, Zhang LQ, Lin WP, Liu WN et al (2014) Overexpressing neuroglobin improves functional recovery by inhibiting neuronal apoptosis after spinal cord injury. Brain Res 1562:100–108. https://doi.org/10.1016/j.brainres.2014.03.020
27. Lechauve C, Augustin S, Roussel D, Sahel JA, Corral-Debrinski M (2013) Neuroglobin involvement in visual pathways through the optic nerve. Biochim Biophys Acta 1834(9):1772–1778. https://doi.org/10.1016/j.bbapap.2013.04.014
28. Avivi A, Gerlach F, Joel A, Reuss S, Burmester T, Nevo E, Hankeln T (2010) Neuroglobin, cytoglobin, and myoglobin contribute to hypoxia adaptation of the subterranean mole rat Spalax. Proc Natl Acad Sci U S A 107(50):21570–21575. https://doi.org/10.1073/pnas.1015379107
29. Zhao S, Yu Z, Zhao G, Xing C, Hayakawa K, Whalen MJ, Lok JM, Lo EH et al (2012) Neuroglobin-overexpression reduces traumatic brain lesion size in mice. BMC Neurosci 13:67. https://doi.org/10.1186/1471-2202-13-67
30. Yu Z, Liu N, Liu J, Yang K, Wang X (2012) Neuroglobin, a novel target for endogenous neuroprotection against stroke and neurodegenerative disorders. Int J Mol Sci 13(6):6995–7014. https://doi.org/10.3390/ijms13066995
31. Taylor JM, Kelley B, Gregory EJ, Berman NE (2014) Neuroglobin overexpression improves sensorimotor outcomes in a mouse model of traumatic brain injury. Neurosci Lett 577:125–129. https://doi.org/10.1016/j.neulet.2014.03.012
32. Zhou Z, Chen Y, Zhang H, Min S, Yu B, He B, Jin A (2013) Comparison of mesenchymal stromal cells from human bone marrow and adipose tissue for the treatment of spinal cord injury. Cytotherapy 15(4):434–448. https://doi.org/10.1016/j.jcyt.2012.11.015
33. Avila-Rodriguez M, Garcia-Segura LM, Hidalgo-Lanussa O, Baez E, Gonzalez J, Barreto GE (2016) Tibolone protects astrocytic cells from glucose deprivation through a mechanism involving estrogen receptor beta and the upregulation of neuroglobin expression. Mol Cell Endocrinol 433:35–46. https://doi.org/10.1016/j.mce.2016.05.024
34. Sasaki S, Futagi Y, Kobayashi M, Ogura J, Iseki K (2015) Functional characterization of 5-oxoproline transport via SLC16A1/MCT1. J Biol Chem 290(4):2303–2311. https://doi.org/10.1074/jbc.M114.581892
35. Cabezas R, Avila MF, Gonzalez J, El-Bacha RS, Barreto GE (2015) PDGF-BB protects mitochondria from rotenone in T98G

cells. Neurotox Res 27(4):355–367. https://doi.org/10.1007/s12640-014-9509-5
36. Mimura J, Kosaka K, Maruyama A, Satoh T, Harada N, Yoshida H, Satoh K, Yamamoto M et al (2011) Nrf2 regulates NGF mRNA induction by carnosic acid in T98G glioblastoma cells and normal human astrocytes. J Biochem 150(2):209–217. https://doi.org/10.1093/jb/mvr065
37. Bourguignon LY, Gilad E, Peyrollier K, Brightman A, Swanson RA (2007) Hyaluronan-CD44 interaction stimulates Rac1 signaling and PKN gamma kinase activation leading to cytoskeleton function and cell migration in astrocytes. J Neurochem 101(4):1002–1017. https://doi.org/10.1111/j.1471-4159.2007.04485.x
38. Ouyang YB, Xu LJ, Emery JF, Lee AS, Giffard RG (2011) Overexpressing GRP78 influences Ca2+ handling and function of mitochondria in astrocytes after ischemia-like stress. Mitochondrion 11(2):279–286. https://doi.org/10.1016/j.mito.2010.10.007
39. Vomelova I, Vaníčková Z, Šedo A (2009) Technical note methods of RNA purification. All ways (should) lead to Rome. Folia Biologica (Praha) 55:243–251
40. Scientific TF (2015) Real-time PCR Solutions.
41. Taylor SC, Berkelman T, Yadav G, Hammond M (2013) A defined methodology for reliable quantification of Western blot data. Mol Biotechnol 55(3):217–226. https://doi.org/10.1007/s12033-013-9672-6
42. Gassmann M, Grenacher B, Rohde B, Vogel J (2009) Quantifying Western blots: pitfalls of densitometry. Electrophoresis 30(11):1845–1855. https://doi.org/10.1002/elps.200800720
43. Voloboueva LA, Lee SW, Emery JF, Palmer TD, Giffard RG (2010) Mitochondrial protection attenuates inflammation-induced impairment of neurogenesis in vitro and in vivo. J Neurosci 30(37):12242–12251. https://doi.org/10.1523/JNEUROSCI.1752-10.2010
44. Cassina P, Cassina A, Pehar M, Castellanos R, Gandelman M, de Leon A, Robinson KM, Mason RP et al (2008) Mitochondrial dysfunction in SOD1G93A-bearing astrocytes promotes motor neuron degeneration: prevention by mitochondrial-targeted antioxidants. J Neurosci 28(16):4115–4122. https://doi.org/10.1523/JNEUROSCI.5308-07.2008
45. Wang H, Joseph JA (1999) Quantifying cellular oxidative stress by dichlorofluorescein assay using microplate reader. Free Radic Biol Med 27(5–6):612–616
46. Alarifi S, Ali D, Alkahtani S (2015) Nanoalumina induces apoptosis by impairing antioxidant enzyme systems in human hepatocarcinoma cells. Int J Nanomedicine 10:3751–3760. https://doi.org/10.2147/IJN.S82050
47. Pokrzywinski KL, Tilney CL, Warner ME, Coyne KJ (2017) Cell cycle arrest and biochemical changes accompanying cell death in harmful dinoflagellates following exposure to bacterial algicide IRI-160AA. Sci Rep 7:45102. https://doi.org/10.1038/srep45102
48. Jeong SH, Kim HK, Song IS, Noh SJ, Marquez J, Ko KS, Rhee BD, Kim N et al (2014) Echinochrome a increases mitochondrial mass and function by modulating mitochondrial biogenesis regulatory genes. Marine Drugs 12(8):4602–4615. https://doi.org/10.3390/md12084602
49. Oliva CR, Moellering DR, Gillespie GY, Griguer CE (2011) Acquisition of chemoresistance in gliomas is associated with increased mitochondrial coupling and decreased ROS production. PLoS One 6(9):e24665. https://doi.org/10.1371/journal.pone.0024665
50. Hidalgo-Lanussa O, Avila-Rodriguez M, Baez-Jurado E, Zamudio J, Echeverria V, Garcia-Segura LM, Barreto GE (2018) Tibolone reduces oxidative damage and inflammation in microglia stimulated with palmitic acid through mechanisms involving estrogen receptor beta. Mol Neurobiol 55(7):5462–5477. https://doi.org/10.1007/s12035-017-0777-y
51. Li Q, Lau A, Morris TJ, Guo L, Fordyce CB, Stanley EF (2004) A syntaxin 1, Galpha(o), and N-type calcium channel complex at a presynaptic nerve terminal: analysis by quantitative immunocolocalization. J Neurosci 24(16):4070–4081. https://doi.org/10.1523/JNEUROSCI.0346-04.2004
52. Amor S, Puentes F, Baker D, van der Valk P (2010) Inflammation in neurodegenerative diseases. Immunology 129(2):154–169. https://doi.org/10.1111/j.1365-2567.2009.03225.x
53. Stephenson J, Nutma E, van der Valk P, Amor S (2018) Inflammation in CNS neurodegenerative diseases. Immunology 154(2):204–219. https://doi.org/10.1111/imm.12922
54. Kokiko-Cochran ON, Godbout JP (2018) The inflammatory continuum of traumatic brain injury and Alzheimer's disease. Front Immunol 9:672. https://doi.org/10.3389/fimmu.2018.00672
55. Chung WS, Allen NJ, Eroglu C (2015) Astrocytes control synapse formation, function, and elimination. Cold Spring Harb Perspect Biol 7(9):a020370. https://doi.org/10.1101/cshperspect.a020370
56. Becerra-Calixto A, Cardona-Gomez GP (2017) The role of astrocytes in neuroprotection after brain stroke: potential in cell therapy. Front Mol Neurosci 10:88. https://doi.org/10.3389/fnmol.2017.00088
57. Kimelberg HK, Nedergaard M (2010) Functions of astrocytes and their potential as therapeutic targets. Neurotherapeutics 7(4):338–353. https://doi.org/10.1016/j.nurt.2010.07.006
58. Cekanaviciute E, Buckwalter MS (2016) Astrocytes: integrative regulators of neuroinflammation in stroke and other neurological diseases. Neurotherapeutics 13(4):685–701. https://doi.org/10.1007/s13311-016-0477-8
59. Colombo E, Farina C (2016) Astrocytes: key regulators of neuroinflammation. Trends Immunol 37(9):608–620. https://doi.org/10.1016/j.it.2016.06.006
60. Le Thuc O, Blondeau N, Nahon JL, Rovere C (2015) The complex contribution of chemokines to neuroinflammation: switching from beneficial to detrimental effects. Ann N Y Acad Sci 1351:127–140. https://doi.org/10.1111/nyas.12855
61. Kempuraj D, Thangavel R, Selvakumar GP, Zaheer S, Ahmed ME, Raikwar SP, Zahoor H, Saeed D et al (2017) Brain and peripheral atypical inflammatory mediators potentiate neuroinflammation and neurodegeneration. Front Cell Neurosci 11:216. https://doi.org/10.3389/fncel.2017.00216
62. Cunningham CJ, Redondo-Castro E, Allan SM (2018) The therapeutic potential of the mesenchymal stem cell secretome in ischaemic stroke. Journal of cerebral blood flow and metabolism : official journal of the International Society of Cerebral Blood Flow and Metabolism:271678X18776802. https://doi.org/10.1177/0271678X18776802
63. Valencia J, Blanco B, Yanez R, Vazquez M, Herrero Sanchez C, Fernandez-Garcia M, Rodriguez Serrano C, Pescador D et al (2016) Comparative analysis of the immunomodulatory capacities of human bone marrow- and adipose tissue-derived mesenchymal stromal cells from the same donor. Cytotherapy 18(10):1297–1311. https://doi.org/10.1016/j.jcyt.2016.07.006
64. Gimeno ML, Fuertes F, Barcala Tabarrozzi AE, Attorressi AI, Cucchiani R, Corrales L, Oliveira TC, Sogayar MC et al (2017) Pluripotent nontumorigenic adipose tissue-derived muse cells have immunomodulatory capacity mediated by transforming growth factor-beta1. Stem Cells Transl Med 6(1):161–173. https://doi.org/10.5966/sctm.2016-0014
65. Gao F, Chiu SM, Motan DA, Zhang Z, Chen L, Ji HL, Tse HF, Fu QL et al (2016) Mesenchymal stem cells and immunomodulation: current status and future prospects. Cell Death Dis 7:e2062. https://doi.org/10.1038/cddis.2015.327
66. Hariri RJ, Chang VA, Barie PS, Wang RS, Sharif SF, Ghajar JB (1994) Traumatic injury induces interleukin-6 production by human astrocytes. Brain Res 636(1):139–142

67. Liu C, Cui G, Zhu M, Kang X, Guo H (2014) Neuroinflammation in Alzheimer's disease: chemokines produced by astrocytes and chemokine receptors. Int J Clin Exp Pathol 7(12):8342–8355
68. Phuagkhaopong S, Ospondpant D, Kasemsuk T, Sibmooh N, Soodvilai S, Power C, Vivithanaporn P (2017) Cadmium-induced IL-6 and IL-8 expression and release from astrocytes are mediated by MAPK and NF-kappaB pathways. Neurotoxicology 60:82–91. https://doi.org/10.1016/j.neuro.2017.03.001
69. Gijbels K, Van Damme J, Proost P, Put W, Carton H, Billiau A (1990) Interleukin 6 production in the central nervous system during experimental autoimmune encephalomyelitis. Eur J Immunol 20(1):233–235. https://doi.org/10.1002/eji.1830200134
70. Jiang Y, Deacon R, Anthony DC, Campbell SJ (2008) Inhibition of peripheral TNF can block the malaise associated with CNS inflammatory diseases. Neurobiol Dis 32(1):125–132. https://doi.org/10.1016/j.nbd.2008.06.017
71. Lucas SM, Rothwell NJ, Gibson RM (2006) The role of inflammation in CNS injury and disease. Br J Pharmacol 147(Suppl 1):S232–S240. https://doi.org/10.1038/sj.bjp.0706400
72. Tehranian R, Andell-Jonsson S, Beni SM, Yatsiv I, Shohami E, Bartfai T, Lundkvist J, Iverfeldt K (2002) Improved recovery and delayed cytokine induction after closed head injury in mice with central overexpression of the secreted isoform of the interleukin-1 receptor antagonist. J Neurotrauma 19(8):939–951. https://doi.org/10.1089/089771502320317096
73. Guida E, Stewart A (1998) Influence of hypoxia and glucose deprivation on tumour necrosis factor-alpha and granulocyte-macrophage colony-stimulating factor expression in human cultured monocytes. Cell Physiol Biochem 8(1–2):75–88. https://doi.org/10.1159/000016272
74. Opal SM, DePalo VA (2000) Anti-inflammatory cytokines. Chest 117(4):1162–1172
75. Xia W, Peng GY, Sheng JT, Zhu FF, Guo JF, Chen WQ (2015) Neuroprotective effect of interleukin-6 regulation of voltage-gated Na(+) channels of cortical neurons is time- and dose-dependent. Neural Regen Res 10(4):610–617. https://doi.org/10.4103/1673-5374.155436
76. Erta M, Quintana A, Hidalgo J (2012) Interleukin-6, a major cytokine in the central nervous system. Int J Biol Sci 8(9):1254–1266. https://doi.org/10.7150/ijbs.4679
77. Jiang T, Cadenas E (2014) Astrocytic metabolic and inflammatory changes as a function of age. Aging Cell 13(6):1059–1067. https://doi.org/10.1111/acel.12268
78. Chen XL, Wang Y, Peng WW, Zheng YJ, Zhang TN, Wang PJ, Huang JD, Zeng QY (2018) Effects of interleukin-6 and IL-6/AMPK signaling pathway on mitochondrial biogenesis and astrocytes viability under experimental septic condition. Int Immunopharmacol 59:287–294. https://doi.org/10.1016/j.intimp.2018.04.020
79. Jiang CL, Lu CL (1998) Interleukin-2 and its effects in the central nervous system. Biol Signals Recept 7(3):148–156. https://doi.org/10.1159/000014541
80. Xie L, Choudhury GR, Winters A, Yang SH, Jin K (2015) Cerebral regulatory T cells restrain microglia/macrophage-mediated inflammatory responses via IL-10. Eur J Immunol 45(1):180–191. https://doi.org/10.1002/eji.201444823
81. Bhela S, Varanasi SK, Jaggi U, Sloan SS, Rajasagi NK, Rouse BT (2017) The plasticity and stability of regulatory T cells during viral-induced inflammatory lesions. J Immunol 199(4):1342–1352. https://doi.org/10.4049/jimmunol.1700520
82. Rothhammer V, Quintana FJ (2015) Control of autoimmune CNS inflammation by astrocytes. Semin Immunopathol 37(6):625–638. https://doi.org/10.1007/s00281-015-0515-3
83. Bajetto A, Bonavia R, Barbero S, Schettini G (2002) Characterization of chemokines and their receptors in the central nervous system: physiopathological implications. J Neurochem 82(6):1311–1329
84. Hao P, Liang Z, Piao H, Ji X, Wang Y, Liu Y, Liu R, Liu J (2014) Conditioned medium of human adipose-derived mesenchymal stem cells mediates protection in neurons following glutamate excitotoxicity by regulating energy metabolism and GAP-43 expression. Metab Brain Dis 29(1):193–205. https://doi.org/10.1007/s11011-014-9490-y
85. Bruno V, Copani A, Besong G, Scoto G, Nicoletti F (2000) Neuroprotective activity of chemokines against N-methyl-D-aspartate or beta-amyloid-induced toxicity in culture. Eur J Pharmacol 399(2–3):117–121
86. Mamik MK, Ghorpade A (2016) CXCL8 as a potential therapeutic target for HIV-associated neurocognitive disorders. Curr Drug Targets 17(1):111–121
87. Meiron M, Zohar Y, Anunu R, Wildbaum G, Karin N (2008) CXCL12 (SDF-1alpha) suppresses ongoing experimental autoimmune encephalomyelitis by selecting antigen-specific regulatory T cells. J Exp Med 205(11):2643–2655. https://doi.org/10.1084/jem.20080730
88. Chaudhry H, Zhou J, Zhong Y, Ali MM, McGuire F, Nagarkatti PS, Nagarkatti M (2013) Role of cytokines as a double-edged sword in sepsis. In Vivo 27(6):669–684
89. Linero I, Chaparro O (2014) Paracrine effect of mesenchymal stem cells derived from human adipose tissue in bone regeneration. PLoS One 9(9):e107001. https://doi.org/10.1371/journal.pone.0107001
90. Kilroy GE, Foster SJ, Wu X, Ruiz J, Sherwood S, Heifetz A, Ludlow JW, Stricker DM et al (2007) Cytokine profile of human adipose-derived stem cells: expression of angiogenic, hematopoietic, and pro-inflammatory factors. J Cell Physiol 212(3):702–709. https://doi.org/10.1002/jcp.21068
91. Wei X, Du Z, Zhao L, Feng D, Wei G, He Y, Tan J, Lee WH et al (2009) IFATS collection: the conditioned media of adipose stromal cells protect against hypoxia-ischemia-induced brain damage in neonatal rats. Stem Cells 27(2):478–488. https://doi.org/10.1634/stemcells.2008-0333
92. Kupcova Skalnikova H (2013) Proteomic techniques for characterisation of mesenchymal stem cell secretome. Biochimie 95(12):2196–2211. https://doi.org/10.1016/j.biochi.2013.07.015
93. Deng LX, Hu J, Liu N, Wang X, Smith GM, Wen X, Xu XM (2011) GDNF modifies reactive astrogliosis allowing robust axonal regeneration through Schwann cell-seeded guidance channels after spinal cord injury. Exp Neurol 229(2):238–250. https://doi.org/10.1016/j.expneurol.2011.02.001
94. Cirillo G, Bianco MR, Colangelo AM, Cavaliere C, Daniele de L, Zaccaro L, Alberghina L, Papa M (2011) Reactive astrocytosis-induced perturbation of synaptic homeostasis is restored by nerve growth factor. Neurobiol Dis 41(3):630–639. https://doi.org/10.1016/j.nbd.2010.11.012
95. Dimitrov DH, Lee S, Yantis J, Honaker C, Braida N (2014) Cytokine serum levels as potential biological markers for the psychopathology in schizophrenia. Adv Psychiatry 2014:1–7
96. Holliday J, Gruol DL (1993) Cytokine stimulation increases intracellular calcium and alters the response to quisqualate in cultured cortical astrocytes. Brain Res 621(2):233–241
97. Galic MA, Riazi K, Pittman QJ (2012) Cytokines and brain excitability. Front Neuroendocrinol 33(1):116–125. https://doi.org/10.1016/j.yfrne.2011.12.002
98. Shinotsuka T, Yasui M, Nuriya M (2014) Astrocytic gap junctional networks suppress cellular damage in an in vitro model of ischemia. Biochem Biophys Res Commun 444(2):171–176. https://doi.org/10.1016/j.bbrc.2014.01.035
99. Helleringer R, Chever O, Daniel H, Galante M (2017) Oxygen and glucose deprivation induces Bergmann glia membrane depolarization and ca(2+) rises mainly mediated by K(+) and ATP

increases in the extracellular space. Front Cell Neurosci 11:349. https://doi.org/10.3389/fncel.2017.00349
100. Reuss B, von Bohlen und Halback O (2003) Fibroblast growth factors and their receptors in the central nervous system. Cell Tissue Res 313(2):139–157. https://doi.org/10.1007/s00441-003-0756-7
101. Wilkins A, Kemp K, Ginty M, Hares K, Mallam E, Scolding N (2009) Human bone marrow-derived mesenchymal stem cells secrete brain-derived neurotrophic factor which promotes neuronal survival in vitro. Stem Cell Res 3(1):63–70. https://doi.org/10.1016/j.scr.2009.02.006
102. Papazian I, Kyrargyri V, Evangelidou M, Voulgari-Kokota A, Probert L (2018) Mesenchymal stem cell protection of neurons against glutamate excitotoxicity involves reduction of NMDA-triggered calcium responses and surface GluR1, and is partly mediated by TNF. Int J Mol Sci 19 (3). https://doi.org/10.3390/ijms19030651
103. Taoufik E, Valable S, Muller GJ, Roberts ML, Divoux D, Tinel A, Voulgari-Kokota A, Tseveleki V et al (2007) FLIP(L) protects neurons against in vivo ischemia and in vitro glucose deprivation-induced cell death. J Neurosci 27(25):6633–6646. https://doi.org/10.1523/JNEUROSCI.1091-07.2007
104. Marchetti L, Klein M, Schlett K, Pfizenmaier K, Eisel UL (2004) Tumor necrosis factor (TNF)-mediated neuroprotection against glutamate-induced excitotoxicity is enhanced by N-methyl-D-aspartate receptor activation. Essential role of a TNF receptor 2-mediated phosphatidylinositol 3-kinase-dependent NF-kappa B pathway. J Biol Chem 279(31):32869–32881. https://doi.org/10.1074/jbc.M311766200
105. Probert L (2015) TNF and its receptors in the CNS: the essential, the desirable and the deleterious effects. Neuroscience 302:2–22. https://doi.org/10.1016/j.neuroscience.2015.06.038
106. Morales AP, Carvalho AC, Monteforte PT, Hirata H, Han SW, Hsu YT, Smaili SS (2011) Endoplasmic reticulum calcium release engages Bax translocation in cortical astrocytes. Neurochem Res 36(5):829–838. https://doi.org/10.1007/s11064-011-0411-8
107. Verkhratsky A, Rodriguez JJ, Parpura V (2012) Calcium signalling in astroglia. Mol Cell Endocrinol 353(1–2):45–56. https://doi.org/10.1016/j.mce.2011.08.039
108. Johnson GG, White MC, Wu JH, Vallejo M, Grimaldi M (2014) The deadly connection between endoplasmic reticulum, Ca2+, protein synthesis, and the endoplasmic reticulum stress response in malignant glioma cells. Neuro-Oncology 16(8):1086–1099. https://doi.org/10.1093/neuonc/nou012
109. Begum G, Kintner D, Liu Y, Cramer SW, Sun D (2012) DHA inhibits ER Ca2+ release and ER stress in astrocytes following in vitro ischemia. J Neurochem 120(4):622–630. https://doi.org/10.1111/j.1471-4159.2011.07606.x
110. Hajnoczky G, Robb-Gaspers LD, Seitz MB, Thomas AP (1995) Decoding of cytosolic calcium oscillations in the mitochondria. Cell 82(3):415–424
111. Reyes RC, Parpura V (2008) Mitochondria modulate Ca2+−dependent glutamate release from rat cortical astrocytes. J Neurosci 28(39):9682–9691. https://doi.org/10.1523/JNEUROSCI.3484-08.2008
112. Parpura V, Grubisic V, Verkhratsky A (2011) Ca(2+) sources for the exocytotic release of glutamate from astrocytes. Biochim Biophys Acta 1813(5):984–991. https://doi.org/10.1016/j.bbamcr.2010.11.006
113. Voulgari-Kokota A, Fairless R, Karamita M, Kyrargyri V, Tseveleki V, Evangelidou M, Delorme B, Charbord P et al (2012) Mesenchymal stem cells protect CNS neurons against glutamate excitotoxicity by inhibiting glutamate receptor expression and function. Exp Neurol 236(1):161–170. https://doi.org/10.1016/j.expneurol.2012.04.011
114. Cheng B, Furukawa K, O'Keefe JA, Goodman Y, Kihiko M, Fabian T, Mattson MP (1995) Basic fibroblast growth factor selectively increases AMPA-receptor subunit GluR1 protein level and differentially modulates Ca2+ responses to AMPA and NMDA in hippocampal neurons. J Neurochem 65(6):2525–2536
115. Ranieri M, Brajkovic S, Riboldi G, Ronchi D, Rizzo F, Bresolin N, Corti S, Comi GP (2013) Mitochondrial fusion proteins and human diseases. Neurol Res Int 2013:293893. https://doi.org/10.1155/2013/293893
116. Burte F, Carelli V, Chinnery PF, Yu-Wai-Man P (2015) Disturbed mitochondrial dynamics and neurodegenerative disorders. Nat Rev Neurol 11(1):11–24. https://doi.org/10.1038/nrneurol.2014.228
117. Qi X, Disatnik MH, Shen N, Sobel RA, Mochly-Rosen D (2011) Aberrant mitochondrial fission in neurons induced by protein kinase C{delta} under oxidative stress conditions in vivo. Mol Biol Cell 22(2):256–265. https://doi.org/10.1091/mbc.E10-06-0551
118. Stojanovski D, Koutsopoulos OS, Okamoto K, Ryan MT (2004) Levels of human Fis1 at the mitochondrial outer membrane regulate mitochondrial morphology. J Cell Sci 117(Pt 7):1201–1210. https://doi.org/10.1242/jcs.01058
119. Elgass K, Pakay J, Ryan MT, Palmer CS (2013) Recent advances into the understanding of mitochondrial fission. Biochim Biophys Acta 1833(1):150–161. https://doi.org/10.1016/j.bbamcr.2012.05.002
120. Szabadkai G, Simoni AM, Bianchi K, De Stefani D, Leo S, Wieckowski MR, Rizzuto R (2006) Mitochondrial dynamics and Ca2+ signaling. Biochim Biophys Acta 1763(5–6):442–449. https://doi.org/10.1016/j.bbamcr.2006.04.002
121. Bravo-Sagua R, Parra V, Lopez-Crisosto C, Diaz P, Quest AF, Lavandero S (2017) Calcium transport and signaling in mitochondria. Comp Physiol 7(2):623–634. https://doi.org/10.1002/cphy.c160013
122. Ogunbileje JO, Porter C, Herndon DN, Chao T, Abdelrahman DR, Papadimitriou A, Chondronikola M, Zimmers TA et al (2016) Hypermetabolism and hypercatabolism of skeletal muscle accompany mitochondrial stress following severe burn trauma. Am J Phys Endocrinol Metab 311(2):E436–E448. https://doi.org/10.1152/ajpendo.00535.2015
123. Eisner V, Picard M, Hajnóczky G (2018) Mitochondrial dynamics in adaptive and maladaptive cellular stress responses. Nat Cell Biol 1
124. Tondera D, Grandemange S, Jourdain A, Karbowski M, Mattenberger Y, Herzig S, Da Cruz S, Clerc P et al (2009) SLP-2 is required for stress-induced mitochondrial hyperfusion. EMBO J 28(11):1589–1600. https://doi.org/10.1038/emboj.2009.89
125. Jagasia R, Grote P, Westermann B, Conradt B (2005) DRP-1-mediated mitochondrial fragmentation during EGL-1-induced cell death in C. elegans. Nature 433(7027):754–760. https://doi.org/10.1038/nature03316
126. Fannjiang Y, Cheng WC, Lee SJ, Qi B, Pevsner J, McCaffery JM, Hill RB, Basanez G et al (2004) Mitochondrial fission proteins regulate programmed cell death in yeast. Genes Dev 18(22):2785–2797. https://doi.org/10.1101/gad.1247904
127. Chang CR, Blackstone C (2010) Dynamic regulation of mitochondrial fission through modification of the dynamin-related protein Drp1. Ann N Y Acad Sci 1201:34–39. https://doi.org/10.1111/j.1749-6632.2010.05629.x
128. Alavi MV, Fuhrmann N (2013) Dominant optic atrophy, OPA1, and mitochondrial quality control: understanding mitochondrial network dynamics. Mol Neurodegener 8:32. https://doi.org/10.1186/1750-1326-8-32
129. Mishra P, Chan DC (2016) Metabolic regulation of mitochondrial dynamics. J Cell Biol 212(4):379–387. https://doi.org/10.1083/jcb.201511036

130. Gomes LC, Di Benedetto G, Scorrano L (2011) During autophagy mitochondria elongate, are spared from degradation and sustain cell viability. Nat Cell Biol 13(5):589–598. https://doi.org/10.1038/ncb2220
131. Lee YJ, Jeong SY, Karbowski M, Smith CL, Youle RJ (2004) Roles of the mammalian mitochondrial fission and fusion mediators Fis1, Drp1, and Opa1 in apoptosis. Mol Biol Cell 15(11):5001–5011. https://doi.org/10.1091/mbc.e04-04-0294
132. Cereghetti GM, Costa V, Scorrano L (2010) Inhibition of Drp1-dependent mitochondrial fragmentation and apoptosis by a polypeptide antagonist of calcineurin. Cell Death Differ 17(11):1785–1794. https://doi.org/10.1038/cdd.2010.61
133. Frank S, Gaume B, Bergmann-Leitner ES, Leitner WW, Robert EG, Catez F, Smith CL, Youle RJ (2001) The role of dynamin-related protein 1, a mediator of mitochondrial fission, in apoptosis. Dev Cell 1(4):515–525
134. Frezza C, Cipolat S, Martins de Brito O, Micaroni M, Beznoussenko GV, Rudka T, Bartoli D, Polishuck RS et al (2006) OPA1 controls apoptotic cristae remodeling independently from mitochondrial fusion. Cell 126(1):177–189. https://doi.org/10.1016/j.cell.2006.06.025
135. Elachouri G, Vidoni S, Zanna C, Pattyn A, Boukhaddaoui H, Gaget K, Yu-Wai-Man P, Gasparre G et al (2011) OPA1 links human mitochondrial genome maintenance to mtDNA replication and distribution. Genome Res 21(1):12–20. https://doi.org/10.1101/gr.108696.110
136. Olichon A, Baricault L, Gas N, Guillou E, Valette A, Belenguer P, Lenaers G (2003) Loss of OPA1 perturbates the mitochondrial inner membrane structure and integrity, leading to cytochrome c release and apoptosis. J Biol Chem 278(10):7743–7746. https://doi.org/10.1074/jbc.C200677200
137. Mizushima N (2005) The pleiotropic role of autophagy: from protein metabolism to bactericide. Cell Death Differ 12(Suppl 2):1535–1541. https://doi.org/10.1038/sj.cdd.4401728
138. Klionsky DJ, Emr SD (2000) Autophagy as a regulated pathway of cellular degradation. Science 290(5497):1717–1721
139. Wu YT, Tan HL, Huang Q, Kim YS, Pan N, Ong WY, Liu ZG, Ong CN et al (2008) Autophagy plays a protective role during zVAD-induced necrotic cell death. Autophagy 4(4):457–466
140. Cecconi F, Levine B (2008) The role of autophagy in mammalian development: cell makeover rather than cell death. Dev Cell 15(3):344–357. https://doi.org/10.1016/j.devcel.2008.08.012
141. White KE, Davies VJ, Hogan VE, Piechota MJ, Nichols PP, Turnbull DM, Votruba M (2009) OPA1 deficiency associated with increased autophagy in retinal ganglion cells in a murine model of dominant optic atrophy. Invest Ophthalmol Vis Sci 50(6):2567–2571. https://doi.org/10.1167/iovs.08-2913
142. Kane MS, Alban J, Desquiret-Dumas V, Gueguen N, Ishak L, Ferre M, Amati-Bonneau P, Procaccio V et al (2017) Autophagy controls the pathogenicity of OPA1 mutations in dominant optic atrophy. J Cell Mol Med 21(10):2284–2297. https://doi.org/10.1111/jcmm.13149
143. Gomes LC, Scorrano L (2011) Mitochondrial elongation during autophagy: a stereotypical response to survive in difficult times. Autophagy 7(10):1251–1253. https://doi.org/10.4161/auto.7.10.16771
144. Gomes LC, Scorrano L (2013) Mitochondrial morphology in mitophagy and macroautophagy. Biochim Biophys Acta 1833(1):205–212. https://doi.org/10.1016/j.bbamcr.2012.02.012
145. Hackenbrock CR (1968) Chemical and physical fixation of isolated mitochondria in low-energy and high-energy states. Proc Natl Acad Sci U S A 61(2):598–605
146. Pidoux G, Witczak O, Jarnaess E, Myrvold L, Urlaub H, Stokka AJ, Kuntziger T, Tasken K (2011) Optic atrophy 1 is an A-kinase anchoring protein on lipid droplets that mediates adrenergic control of lipolysis. EMBO J 30(21):4371–4386. https://doi.org/10.1038/emboj.2011.365
147. Seo BB, Nakamaru-Ogiso E, Flotte TR, Matsuno-Yagi A, Yagi T (2006) In vivo complementation of complex I by the yeast Ndi1 enzyme. Possible application for treatment of Parkinson disease. J Biol Chem 281(20):14250–14255. https://doi.org/10.1074/jbc.M600922200
148. Marella M, Seo BB, Yagi T, Matsuno-Yagi A (2009) Parkinson's disease and mitochondrial complex I: a perspective on the Ndi1 therapy. J Bioenerg Biomembr 41(6):493–497. https://doi.org/10.1007/s10863-009-9249-z
149. Seo BB, Nakamaru-Ogiso E, Cruz P, Flotte TR, Yagi T, Matsuno-Yagi A (2004) Functional expression of the single subunit NADH dehydrogenase in mitochondria in vivo: a potential therapy for complex I deficiencies. Hum Gene Ther 15(9):887–895. https://doi.org/10.1089/hum.2004.15.887
150. Yu Z, Zhang Y, Liu N, Yuan J, Lin L, Zhuge Q, Xiao J, Wang X (2016) Roles of neuroglobin binding to mitochondrial complex III subunit cytochrome c1 in oxygen-glucose deprivation-induced neurotoxicity in primary neurons. Mol Neurobiol 53(5):3249–3257. https://doi.org/10.1007/s12035-015-9273-4
151. Ma WW, Hou CC, Zhou X, Yu HL, Xi YD, Ding J, Zhao X, Xiao R (2013) Genistein alleviates the mitochondria-targeted DNA damage induced by beta-amyloid peptides 25-35 in C6 glioma cells. Neurochem Res 38(7):1315–1323. https://doi.org/10.1007/s11064-013-1019-y
152. Hawkins PT, Anderson KE, Davidson K, Stephens LR (2006) Signalling through class I PI3Ks in mammalian cells. Biochem Soc Trans 34(Pt 5):647–662. https://doi.org/10.1042/BST0340647
153. Anderson CN, Tolkovsky AM (1999) A role for MAPK/ERK in sympathetic neuron survival: protection against a p53-dependent, JNK-independent induction of apoptosis by cytosine arabinoside. J Neurosci 19(2):664–673
154. de Oliveira MR, Ferreira GC, Schuck PF, Dal Bosco SM (2015) Role for the PI3K/Akt/Nrf2 signaling pathway in the protective effects of carnosic acid against methylglyoxal-induced neurotoxicity in SH-SY5Y neuroblastoma cells. Chem Biol Interact 242:396–406. https://doi.org/10.1016/j.cbi.2015.11.003
155. Le Belle JE, Orozco NM, Paucar AA, Saxe JP, Mottahedeh J, Pyle AD, Wu H, Kornblum HI (2011) Proliferative neural stem cells have high endogenous ROS levels that regulate self-renewal and neurogenesis in a PI3K/Akt-dependant manner. Cell Stem Cell 8(1):59–71. https://doi.org/10.1016/j.stem.2010.11.028
156. Zhang Q, Liu G, Wu Y, Sha H, Zhang P, Jia J (2011) BDNF promotes EGF-induced proliferation and migration of human fetal neural stem/progenitor cells via the PI3K/Akt pathway. Molecules 16(12):10146–10156. https://doi.org/10.3390/molecules161210146
157. Zhao J, Cheng YY, Fan W, Yang CB, Ye SF, Cui W, Wei W, Lao LX et al (2015) Botanical drug puerarin coordinates with nerve growth factor in the regulation of neuronal survival and neuritogenesis via activating ERK1/2 and PI3K/Akt signaling pathways in the neurite extension process. CNS Neurosci Ther 21(1):61–70. https://doi.org/10.1111/cns.12334
158. Nguyen TL, Kim CK, Cho JH, Lee KH, Ahn JY (2010) Neuroprotection signaling pathway of nerve growth factor and brain-derived neurotrophic factor against staurosporine induced apoptosis in hippocampal H19-7/IGF-IR [corrected]. Exp Mol Med 42(8):583–595. https://doi.org/10.3858/emm.2010.42.8.060
159. Lotfinia M, Kadivar M, Piryaei A, Pournasr B, Sardari S, Sodeifi N, Sayahpour FA, Baharvand H (2016) Effect of secreted molecules of human embryonic stem cell-derived mesenchymal stem cells on acute hepatic failure model. Stem Cells Dev 25(24):1898–1908. https://doi.org/10.1089/scd.2016.0244

160. Zagoura DS, Roubelakis MG, Bitsika V, Trohatou O, Pappa KI, Kapelouzou A, Antsaklis A, Anagnou NP (2012) Therapeutic potential of a distinct population of human amniotic fluid mesenchymal stem cells and their secreted molecules in mice with acute hepatic failure. Gut 61(6):894–906. https://doi.org/10.1136/gutjnl-2011-300908

161. Toma C, Pittenger MF, Cahill KS, Byrne BJ, Kessler PD (2002) Human mesenchymal stem cells differentiate to a cardiomyocyte phenotype in the adult murine heart. Circulation 105(1):93–98

162. Na HK, Kim EH, Jung JH, Lee HH, Hyun JW, Surh YJ (2008) (−)-Epigallocatechin gallate induces Nrf2-mediated antioxidant enzyme expression via activation of PI3K and ERK in human mammary epithelial cells. Arch Biochem Biophys 476(2):171–177. https://doi.org/10.1016/j.abb.2008.04.003

163. Liu J, Yu Z, Guo S, Lee SR, Xing C, Zhang C, Gao Y, Nicholls DG et al (2009) Effects of neuroglobin overexpression on mitochondrial function and oxidative stress following hypoxia/reoxygenation in cultured neurons. J Neurosci Res 87(1):164–170. https://doi.org/10.1002/jnr.21826

164. Duong TT, Witting PK, Antao ST, Parry SN, Kennerson M, Lai B, Vogt S, Lay PA et al (2009) Multiple protective activities of neuroglobin in cultured neuronal cells exposed to hypoxia reoxygenation injury. J Neurochem 108(5):1143–1154. https://doi.org/10.1111/j.1471-4159.2008.05846.x

165. Yu Z, Xu J, Liu N, Wang Y, Li X, Pallast S, van Leyen K, Wang X (2012) Mitochondrial distribution of neuroglobin and its response to oxygen-glucose deprivation in primary-cultured mouse cortical neurons. Neuroscience 218:235–242. https://doi.org/10.1016/j.neuroscience.2012.05.054

166. Fiocchetti M, Cipolletti M, Leone S, Naldini A, Carraro F, Giordano D, Verde C, Ascenzi P et al (2016) Neuroglobin in breast cancer cells: effect of hypoxia and oxidative stress on protein level, localization, and anti-apoptotic function. PLoS One 11(5):e0154959. https://doi.org/10.1371/journal.pone.0154959

167. De Marinis E, Fiocchetti M, Acconcia F, Ascenzi P, Marino M (2013) Neuroglobin upregulation induced by 17beta-estradiol sequesters cytocrome c in the mitochondria preventing H2O2-induced apoptosis of neuroblastoma cells. Cell Death Dis 4: e508. https://doi.org/10.1038/cddis.2013.30

168. Gorgun FM, Zhuo M, Singh S, Englander EW (2014) Neuroglobin mitigates mitochondrial impairments induced by acute inhalation of combustion smoke in the mouse brain. Inhal Toxicol 26(6):361–369. https://doi.org/10.3109/08958378.2014.902147

169. Cabezas R, Vega-Vela NE, Gonzalez-Sanmiguel J, Gonzalez J, Esquinas P, Echeverria V, Barreto GE (2018) PDGF-BB preserves mitochondrial morphology, attenuates ROS production, and upregulates neuroglobin in an astrocytic model under rotenone insult. Mol Neurobiol 55(4):3085–3095. https://doi.org/10.1007/s12035-017-0567-6

170. Jin K, Mao X, Xie L, Greenberg DA (2012) Interactions between vascular endothelial growth factor and neuroglobin. Neurosci Lett 519(1):47–50. https://doi.org/10.1016/j.neulet.2012.05.018

171. Zhu L, Huang L, Wen Q, Wang T, Qiao L, Jiang L (2017) Recombinant human erythropoietin offers neuroprotection through inducing endogenous erythropoietin receptor and neuroglobin in a neonatal rat model of periventricular white matter damage. Neurosci Lett 650:12–17. https://doi.org/10.1016/j.neulet.2017.03.024